



LUND UNIVERSITY

MRI at 3 T of brain functions and fibre tracts adjacent to intracranial tumors

van Westen, Danielle

2006

[Link to publication](#)

Citation for published version (APA):

van Westen, D. (2006). *MRI at 3 T of brain functions and fibre tracts adjacent to intracranial tumors*. [Doctoral Thesis (compilation), Diagnostic Radiology, (Lund)]. Diagnostisk radiologi, Lunds Universitet.

Total number of authors:

1

General rights

Unless other specific re-use rights are stated the following general rights apply:

Copyright and moral rights for the publications made accessible in the public portal are retained by the authors and/or other copyright owners and it is a condition of accessing publications that users recognise and abide by the legal requirements associated with these rights.

- Users may download and print one copy of any publication from the public portal for the purpose of private study or research.
- You may not further distribute the material or use it for any profit-making activity or commercial gain
- You may freely distribute the URL identifying the publication in the public portal

Read more about Creative commons licenses: <https://creativecommons.org/licenses/>

Take down policy

If you believe that this document breaches copyright please contact us providing details, and we will remove access to the work immediately and investigate your claim.

LUND UNIVERSITY

PO Box 117
221 00 Lund
+46 46-222 00 00

MRI at 3 T of brain functions and fibre tracts adjacent to intracranial tumors

Danielle van Westen

**Akademisk avhandling
som med vederbörligt tillstånd av medicinska Fakulteten vid Lunds Universitet
för avläggande av doktorsexamen i medicinsk vetenskap
kommer att offentligen försvaras**

**Torsdagen den 1 juni 2006, kl 13.00 i Föreläsningssal 3,
Centralblocket, Universitetssjukhuset i Lund**

**Fakultetsopponent: Professor Per Hjalmar Nakstad
Avdelningen för Neuroradiologi 1, Ullevål Universitetssjukhus
Oslo, Norge**

**Institutionen för kliniska vetenskaper, Lund
Diagnostisk Radiologi
Universitetssjukhuset i Lund**

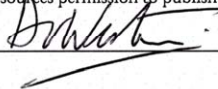


**LUNDS
UNIVERSITET**
Medicinska fakulteten

Organization LUND UNIVERSITY Department of Clinical Sciences, Lund Diagnostic radiology Lund University Hospital 221 85 Lund		Document name DOCTORAL DISSERTATION	
		Date of issue June 1, 2006	
Author(s) Danielle van Westen		Sponsoring organization	
Title and subtitle MRI at 3 T of brain functions and fibre tracts adjacent to intracranial tumors			
Abstract Aims of the studies: • to evaluate the spatial resolution of fMRI at 3 T by studying fingersomatotopy in area 3 b of the primary sensory area (Paper 1); • to investigate the potential of fMRI at 3T as a clinical tool for preoperative evaluation of patients with intracranial tumors (Paper 2); • to investigate the effect of glioma resection on the spatial extent of fMRI activation as compared to the normal within-subject variability (Paper 3); • to determine whether the apparent diffusion coefficient (ADC) and fractional anisotropy (FA) can distinguish tumor-infiltrated edema in gliomas from pure edema in meningiomas and metastases (Paper 4) Results: • Strict somatotopic organisation in the primary sensory cortex was shown in the group average; at the subject level the thumb was located laterally, anteriorly and inferiorly to the little finger in 94 % of subjects (Paper 1). • The sensorimotor and language areas close to intracranial tumors were identified in 95 % of patients. Paradigm effectiveness ranged from 79 to 95 %. The median quality of the activation maps was high. fMRI contributed to the decision to operate, the surgical approach and the extent of the resection in 9, 13 and 12 patients respectively (Paper 2). • BOLD activations obtained from fMRI with motor, sensory and language stimulation pre- and postoperatively in glioma patients yielded differences in the spatial extent similar to those obtained from repeated examinations in healthy controls (Paper 3). • Values and lesion-to-brain ratios of ADC and FA in peritumoral areas did not differ between high grade gliomas, meningiomas and metastases (Paper 4). Conclusions: Our results suggest that the spatial resolution of fMRI using a clinical protocol is adequate for localisation of the sensory representation of a finger (Paper 1). Preoperative fMRI for mapping of motor, sensory and language functions at 3 T is feasible and contributes to neurosurgical decision making (Paper 2). Longitudinal pre- and postoperative fMRI studies may be performed in patients with gliomas without concerns for potential effects of the decreased tumor volume on the BOLD effect as a possible source of error (Paper 3). Values and lesion-to-brain ratios of ADC and FA may not be useful to distinguish pure edema from tumor-infiltrated edema in peritumoral areas with T2-signal changes (Paper 4).			
Key words: Functional Magnetic Resonance Imaging; somatosensory cortex; neoplasms; diffusion magnetic resonance imaging			
Classification system and/or index terms (if any):			
Supplementary bibliographical information:		Language	
ISSN and key title: 1652-8220		ISBN 91-85481-86-6	
Recipient's notes		Number of pages 97	Price
		Security classification	

Distribution by (name and address)

I, the undersigned, being the copyright owner of the abstract of the above-mentioned dissertation, hereby grant to all reference sources permission to publish and disseminate the abstract of the above-mentioned dissertation.

Signature  Date April 20, 2006

**MRI at 3 T of brain functions and fibre tracts
adjacent to intracranial tumors**

Danielle van Westen

Department of Clinical Sciences, Lund

Diagnostic Radiology

Lund 2006



LUND UNIVERSITY
Faculty of Medicine

Doctoral dissertation 1st June 2006-04-12
Department of Clinical Sciences, Lund
Diagnostic Radiology
Faculty of Medicine
Lund University

Faculty opponent:
Professor Per Hjalmar Nakstad
Department of Neuroradiology
Ullevål University Hospital, Oslo, Norway

Correspondence:
Danielle van Westen
Department of Clinical Sciences, Lund
Diagnostic Radiology
Lund University Hospital
Sweden
e-mail: danielle.van_westen@med.lu.se

Layout and copyright Danielle van Westen (pp 1- 52)
ISSN 1652-8220
ISBN 91-85481-86-6
Printed in Sweden, 2006
Media Tryck, Lund

To my family: Sofie, Nina and Paula

Contents

List of publications	6
Abstract	7
Summary in Swedish	8
Abbreviations	10
Aims of the thesis	11
Introduction	
a. Principles of MRI	12
b. Functional MRI	13
c. DTI	17
d. Intracranial tumors	19
e. The role of MRI in the workup of patients with intracranial tumors	20
Background of the thesis	22
Material and methods	25
Results	29
Discussion	33
Conclusion	40
Acknowledgements	41
References	43

List of publications

1. **Fingersomatotopy in area 3b: an fMRI-study** van Westen D, Fransson P, Olsrud J, Rosen B, Lundborg G, Larsson EM BMC Neurosci. 2004 Aug 20;5:28.
2. **Functional magnetic resonance imaging at 3T as a clinical tool in patients with intracranial tumors** Van Westen D, Skagerberg G, Olsrud J, Fransson P, Larsson EM. Acta Radiol 2005 Oct;46(6):599-609.
3. **The spatial extent of fMRI activation in motor, sensory and language areas does not change after glioma resection** D van Westen, J Olsrud, P Fransson, G Skagerberg, E-M Larsson Submitted to Neuroradiology 20060206
4. **Tumor extension in high grade gliomas assessed with diffusion MRI: values and lesion-to-brain ratios of apparent diffusion coefficient and fractional anisotropy** D. van Westen, J. Lätt, E. Englund, S. Brockstedt, E.-M. Larsson Acta Radiol 2006 April;47(3):311-319

Abstract

The *aims of the studies* were:

- to evaluate the spatial resolution of fMRI at 3 T by studying fingersomatotopy in area 3 b of the primary sensory area (Paper 1);
- to investigate the potential of fMRI at 3T as a clinical tool for preoperative evaluation of patients with intracranial tumors (Paper 2);
- to investigate the effect of glioma resection on the spatial extent of fMRI activation as compared to the normal within-subject variability (Paper 3);
- to determine whether the apparent diffusion coefficient (ADC) and fractional anisotropy (FA) can distinguish tumor-infiltrated edema of gliomas from pure edema of meningiomas and metastases (Paper 4).

Results:

Strict somatotopic organisation in the primary sensory cortex was shown in the group average; at the subject level the thumb was located laterally, anteriorly and inferiorly to the little finger in 94 % of subjects (Paper 1).

The sensorimotor and language areas close to intracranial tumors were identified in 95 % of patients. Paradigm effectiveness ranged from 79 to 95 %. The median quality of the activation maps was high. fMRI contributed to the decision to operate, the surgical approach and the extent of the resection in 9, 13 and 12 patients, respectively (Paper 2).

BOLD activation obtained from fMRI with motor, sensory and language stimulation pre- and postoperatively in glioma patients yielded differences in the spatial extent similar to those obtained from repeated examinations in healthy controls (Paper 3).

Values and lesion-to-brain ratios of ADC and FA in peritumoral edema did not differ between high grade gliomas, meningiomas and metastases (Paper 4).

Conclusions:

Our results suggest that the spatial resolution of fMRI using a clinical protocol is adequate for localisation of the sensory representation of a finger (Paper 1).

Preoperative fMRI for mapping of motor, sensory and language functions at 3 T is feasible and contributes to neurosurgical decision making (Paper 2).

Longitudinal pre- and postoperative fMRI studies may be performed in patients with gliomas without concerns for potential effects of the decreased tumor volume on the BOLD effect as a possible source of error (Paper 3).

Values and lesion-to-brain ratios of ADC and FA may not be useful to distinguish pure edema from tumor-infiltrated edema in peritumoral areas with T2-signal changes (Paper 4).

Key words:

Functional Magnetic Resonance Imaging; somatosensory cortex; neoplasms; diffusion magnetic resonance imaging

Summary in Swedish:

Populärvetenskaplig sammanfattning

Hjärntumörer är relativt vanligt förekommande och antalet nydiagnostiserade fall per år är i ökande. Vid utredning och uppföljning av patienter med misstänkt eller fastställd hjärntumör spelar bildgivande tekniker en betydande roll, med som förstahands metod magnetisk resonanstomografi (MR). Under det senaste decenniet har MR utvecklats från att framställa bilder på hjärnan till att inkludera mätning av fysiologiska variabler, som hjärnans blodflöde (perfusion), vattenmolekylernas rörelse (diffusion) inklusive avbildning av nervbanorna (Diffusion Tensor Imaging, DTI), bestämning av hjärnans kemiska sammansättning (MR spektroskopi, MRS) och mätning av nervcellsaktivitet (funktionell MR, fMRI). Teknikerna är tillgängliga för kliniskt bruk och har fått ytterligare intresse och spridning med introduktionen av MR-kameror med den högre fältstyrka 3 Tesla (T), att jämföra med tidigare gängse 1.5 T. I samband med installationen av 3 T MR-kamera på Neuroröntgen i Lund i januari 2002, kunde fMRI utföras i större utsträckning och med modern teknik. Då initierades detta avhandlingsarbete.

I avhandlingen undersöks värdet av två av dessa tekniker, fMRI och DTI, vid utredningen av hjärntumörer. fMRI mäter ändringar i syresättningen i små blodkärl när nervcellerna aktiveras, exempelvis när handens känselbark stimuleras genom att rytmiskt stryka över handen med ett strävt föremål. Resultatet är en så kallad aktiveringskarta av hjärnan, där varje bildelement färgkodats beroende på dess aktivitetsgrad. Diffusion Tensor Imaging (DTI) är en typ av diffusions MR där vattenmolekylernas rörelse mäts i många riktningar. Metoden ger en uppfattning om huruvida denna rörelse föredrar något riktning i olika vävnader i hjärnan, till exempel sker den i den vita substansen företrädesvis utmed nervbanorna.

I **delarbete 1** undersöktes upplösningen vid fMRI genom att kartlägga fingrarnas representation i area 3 b i den sensoriska barken hos tjugo friska försökspersoner. En strikt ordning, såsom känd från tidigare undersökningar, återfanns på gruppnivå med tummen lokaliserad nedom, framför och vid sidan om lillfingret och däremellan de övriga fingrarna i vanlig ordning. På individnivå återfanns tummen nedom, framför och vid sidan om lillfingret hos 94 % av försökspersonerna och de övriga fingrarna mer utspridda däremellan.

I **delarbete 2** undersöktes tjugo patienter med intrakraniell tumör nära rörelse- och känselbarken eller språkfunktionen preoperativt med fMRI för att kartlägga dessa funktioners läge och bedöma avståndet till tumören. Den funktionen som låg närmast tumören enligt vad kunde förväntas från anatomin, identifierades hos 95 % av patienterna. Stimulering med hand- eller fotrörelse påvisade den motoriska barken hos 90 % av patienterna. Med borstning av hand eller fot påvisades känselbarken hos 95 %. Språkuppgifterna, bilda ord på viss bokstav och rimma, ak

tiverade språkområdena i pann- och tinningloberna i mellan 79 % och 95 % av fallen. Aktiveringskartorna höll hög eller adekvat kvalitet hos 90 % av patienterna. fMRI var av värde för att bedöma huruvida patienten skulle opereras (9 patienter), för att planera operationen tekniskt (13) och för att bestämma operationens omfattning(12).

I **delarbete 3** undersöktes om variationerna i fMRI-aktiviteten efter operation för hjärntumör skiljer sig från variationen hos friska försökspersoner. Sex patienter med gliom undersöktes före operationen samt en vecka och två månader efter operationen; sex friska försökspersoner undersöktes tre upprepade gånger med jämförbart interval. Antalet bildelement som aktiverades vid stimulering av rörelse, känsel och språk i den respektive del av hjärnan bestämdes och låg till grunden för beräkning av ett så kallat lateralitetsindex (LI), där aktiveringen i höger och vänster hjärnhalva jämförs. Variationen hos patienterna skilde sig ej från den hos friska försökspersoner.

I **delarbete 4** undersöktes om två parametrar som kan beräknas från DTI-sekvenser, nämligen apparent diffusion coefficient (ADC) och fractional anisotropy (FA) är av värde för att skilja mellan tumörinfiltrerat ödem hos patienter med gliom och rent ödem hos patienter med meningeom och hjärnmetastaser. Trettio patienter (18 gliom, 7 meningeom och 5 metastaser) inkluderades. ADC och FA bestämdes (a) i området runt tumören med signalökning och (b) på motsvarande ställe i den andra hjärnhalvan. Kvoten mellan området runt tumören och dess motsvarighet i den andra hjärnhalvan beräknades. Någon skillnad i ADC eller FA mellan gliom, meningeom och metastaser framkom inte i varken värde eller kvot.

Sammanfattningsvis talar våra resultat för att ett kliniskt fMRI-protokoll har tillräcklig hög upplösning för att identifiera enstaka fingrar. Preoperativ fMRI med kartläggning av rörelse, känsel och språkfunktionen kan utföras vid 3 T i klinisk miljö med gott resultat och är av värde för den neurokirurgiska bedömningen. Longitudinella fMRI-studier som inkluderar patienter pre- och postoperativt, kan utföras hos gliompatienter utan att resultaten drabbas av variationer i utbredningen av fMRI-aktiviteten. Värden och kvoter av ADC och FA är ej säkert av värde för att skilja mellan tumörinfiltrerat ödem och rent ödem.

Abbreviations

ADC	Apparent Diffusion Coefficient
BOLD	blood oxygen level dependent
CNR	contrast-to-noise ratio
DTI	Diffusion Tensor Imaging
DWI	diffusion weighted imaging
EPI	echoplanar imaging
FA	Fractional Anisotropy
FLAIR	fast fluid attenuated inversion recovery
FOV	field of view
fMRI	functional Magnetic Resonance Imaging
GLM	general linear model
GRE	gradient echo
ICS	intraoperative cortical stimulation
M1	primary motor cortex
MR/MRI	Magnetic Resonance/ Magnetic Resonance Imaging
NAWM	normal appearing white matter
RF	radiofrequency
ROI	region of interest
S1	primary sensory cortex
SE	spin echo
SI	signal intensity
SNR	signal-to-noise ratio
SPM	Statistical Parametric Mapping
T	Tesla
T1 W	T1-weighted
T2 W	T2-weighted
TE	echo time
TI	inversion time
TR	repetition time
WHO	World Health Organisation

Aims of the thesis:

1. To evaluate the spatial resolution of fMRI at 3 T by studying fingersomatotopy in area 3 b of the primary sensory area (Paper 1)
2. To investigate the potential of fMRI at 3T as a clinical tool for preoperative evaluation of patients with intracranial tumors (Paper 2)
3. To investigate the effect of glioma resection on the spatial extent of fMRI activation as compared to the normal within-subject variability (Paper 3)
4. To determine whether the apparent diffusion coefficient (ADC) and fractional anisotropy (FA) can distinguish tumor-infiltrated edema in gliomas from pure edema in meningiomas and metastases (Paper 4)

Introduction

a. Principles of MRI:

The nuclear magnetic resonance (NMR) phenomenon was first described by Bloch and Purcell independently in 1946 [1, 2]. Both were awarded the Nobel Prize in physics in 1952. The NMR imaging technique, later named Magnetic Resonance Imaging (MRI), was first introduced by Lauterbur in 1973 [3], preceded by the observation of characteristic relaxation times in tumors by Damadian in 1971 [4]. The MRI technique is based on the use of a strong magnetic field in combination with radiofrequency (RF) pulses. An MR scanning unit consists of a magnet, additional magnetic field gradients and a radiofrequency coil for transmitting and receiving the MR signal. Image reconstruction requires a high performance computer with appropriate software.

Hydrogen nuclei (protons) exhibit a magnetic property named spin. The protons tend to align themselves parallel to the magnetic field and together form a net magnetisation vector oriented parallel to the main magnetic field. At this point the protons will precess about the field axis at a characteristic frequency with random phase. Application of a brief RF pulse will excite the protons to a higher energy level. The magnetization vector will be tipped away from the direction of the main magnetic field creating a rotating vector component perpendicular to the main magnetic field. This results in the introduction of a transient field coherence. The transverse net magnetisation vector can be detected, since it causes an induced current in a so called receiver coil placed close to it. Immediately after the RF pulse, the protons will return to their original state, thereby reemitting the energy as a radio signal that is dependent on tissue properties and the selected imaging technique. Through the use of gradients applied in three directions, the MR signal can be spatially distributed in volume elements, voxels. However, the signal is weak and can only be observed because of the very large number of protons in the human body. The MR signal always contains some noise and adequate signal to noise (SNR) can be achieved by increasing the main magnetic field strength, averaging multiple measurements and optimally selecting receiver coils for signal detection. MRI provides excellent soft tissue contrast that is determined by the relaxation parameters T1 and T2, proton density, susceptibility effects, diffusion, perfusion, and flow effects. An image can be T1 weighted (T1W) or T2-weighted (T2W) depending on whether the T1- or T2-relaxation properties will dominate the image contrast. The T1- and T2-relaxation times of a tissue reflect the reemission of the energy absorbed from the RF pulse. The T1-relaxation time describes the recovery of the longitudinal magnetisation vector while the T2-relaxation time is dependent on the rate of the signal decay (transverse magnetisation). Two factors contribute to the decay of transverse magnetization: (1) molecular interactions leading to small variations in the local magnetic field, believed to lead to a pure T2 effect and (2) small variations in the external magnetic field and local variation due to particles or tissues with different susceptibilities (e. g. deoxyhemoglobin), believed to lead to an

inhomogeneous T2 effect. The combined time constant is given the symbol T2*. The relationship between the T2 from molecular processes and that from inhomogeneities in the magnetic field is as follows: $1/T2^* = 1/T2 + 1/T2_{inhomo}$. Measurement of the local T2* during task execution is the basis of fMRI.

b. fMRI:

Physiological background:

fMRI provides non-invasive, in vivo mapping of human brain functions by measuring the hemodynamic response in the area of neuronal activity during stimulation and rest. The original idea of neurovascular coupling was introduced by Roy and Sherrington in 1890: “the brain possesses an intrinsic mechanism by which its vascular supply can be varied locally in correspondence with the local variations of functional activity”[5]. The magnetic properties of hemoglobin at its different oxygenation states are responsible for the signal changes measured during fMRI. Deoxygenated hemoglobin is paramagnetic and induces a susceptibility effect in its surroundings by introducing distortions and inhomogeneities in the local magnetic field. Oxyhemoglobin is diamagnetic, which means it has negligible magnetic effect on its surroundings [6]. Activation of a brain area results in increased energy utilisation of its neurons at the synaptic level accompanied by an increase in the regional cerebral blood flow in that area. The increase in blood flow exceeds the increased demand by two- or threefold which results in a local increase of oxyhemoglobin during activation and a relative decrease of deoxyhemoglobin [7]. The result of this neurovascular uncoupling is an increase of the local T2* value and a corresponding increase of the MR signal from the active brain tissue during activation relative to rest [8, 9, 10]. The increase of the MR signal due to a local decrease in the concentration of the paramagnetic deoxyhemoglobin, has been named the blood oxygen level dependent (BOLD)-contrast [11]. Hence, fMRI based on imaging of the BOLD-effect, reflects the synaptic activity of neurons indirectly via MR signal changes due to changes in blood flow, blood volume and blood oxygen concentration in activated areas of the brain. The quantitative relationship of the signal change due to the BOLD-effect and the firing rate of neurons has been shown to be mainly linear [12]. However, the hemodynamic response is sluggish compared to the action potential: following the onset of stimulation, the T2* signal increase due to the BOLD-effect appears after approximately 2 seconds, reaches its maximum after 4-6 seconds and returns to baseline after 10 -12 seconds [13, 14].

Imaging technique:

As mentioned above, loss of the transverse magnetization due to dephasing of the spins under influence of local field inhomogeneities is named the T2* relaxation. As a consequence, the hemodynamic changes generating BOLD-effect, are commonly measured using T2*-weighted measurements. Normally, gradient echo sequences are used because of their lack of refocusing pulse that cancels out the T2* effect. Echo planar imaging (EPI), in turn, offers the acquisition speed required for measuring the BOLD-effect. Data are usually structured in a two-dimensional grid named k-space. In EPI, a single 90 degree RF pulse is used to fill k-space so that one slice may be

imaged in 40 ms and a volume of 36 slices covering the whole brain in 2 seconds or less [15]. A combination of these two techniques, gradient echo echo-planar imaging (GRE-EPI) is the most commonly used sequence for fMRI.

The MRI signal always contains noise due to movement of charged particles in the body and small anomalies in the measurement electronics. The signal-to-noise ratio (SNR) of an image is defined in terms of the variation of values within the image of a uniform test object and is ideally calculated as the ratio of the average MRI signal to the standard deviation of the noise. The determination of the average value requires a region of interest (ROI) placed in tissue with high signal intensity (e. g., white matter in the corpus callosum). The noise is measured by means of a ROI placed outside the object in the image background. The SNR is proportional to the field strength and dependent on magnet shimming, parameters included in the sequence (TR, TE, T1, T2, flip angle and bandwidth), voxel volume, and coil sensitivity [16, 17]. For fMRI, the ratio of activation-related signal change to the noise component of the signal, often referred to as the contrast-to-noise ratio or CNR, is a relevant parameter. CNR is obtained by dividing the difference in signal intensity between activation (A) and rest (R) by the background noise (N) : $CNR = S(A) - S(R) / N$. Since the relationship between field strength and SNR is linear, SNR will approximately double when going from 1.5 T to 3 T. As the SNR increases, the CNR also increases approximately linearly [18]. BOLD imaging gains an additional boost from increased field strength because susceptibility effects generally increase with the square of the field strength. Hence, at 3 T, the level of signal increase between activation and rest can be up to 4%, compared with 2% or less at 1.5 T [19].

Experimental design:

The simplest fMRI experiment uses a sensorimotor or cognitive task (e. g. fingertapping, word generation) and a resting task that may involve the viewing of a cross. During one ‘run’ these two tasks are alternated in a so called ‘on-off’ or ‘block-design’ while rapid imaging is performed continuously. The optimal duration of a task allowing for measurement of the hemodynamic response without habituation or fatigue effects occurring, is considered to be 20-40 seconds. In order to achieve acceptable CNR, several repetitions of both tasks are performed in one run.

Image processing:

The processing of functional image volumes involves a number of steps, often performed using software packages such as SPM (Statistical Parametric Mapping) or Brain Voyager [20, 21].

Correction for head motion is essential for fMRI data because the change in signal intensity between activation and rest may be smaller than signal intensity variations due to head motion. Motion correction often involves rigid alignment of the consecutively acquired images with the first image using a least-square approach which may be performed in real-time during image acquisition [22].

Coregistration implies aligning of the functional volumes and the anatomical data set in space so that activation can be overlaid on an image with high resolution.

Smoothing is a process by which data points are averaged with their neighbours. The effect is a blurring of the sharp edges in the smoothed data. Smoothing is sometimes referred to as filtering, because it suppresses high frequency signal and enhances low frequency signal such as the BOLD-effect. Smoothing will result in increased signal-to-noise in the data and thus lead to improved sensitivity to potential effects. In addition it reduces the number of independent observations, by averaging values across voxels.

Statistical analysis:

The image volumes acquired during an fMRI study consist of volume elements, named voxels. The measured parameter is the signal intensity in each voxel, which has been determined for each TR. The signal intensity within a given voxel in an activated area will vary in response to the stimulus in our paradigm. The analysis aims at identifying areas in the brain which show an effect of stimulation using a statistical test. In software packages like SPM or Brain Voyager this analysis is performed for each voxel individually and simultaneously.

In SPM, the general linear model (GLM) is used to analyze the variance of the signal intensity using multiple regression [23, 24]. The first step involves computing statistics that give evidence supporting the rejection of the null hypothesis (i.e. that there is no effect of stimulation). The signal intensity over time is our observed response variable Y_j , where $j=1, \dots, J$ indexes the observation. Suppose that we have a set of L explanatory variables denoted by x_{jl} , where $l = 1, \dots, L$ indexes the explanatory variables. The GLM explains the response variable in terms of a linear combination of the explanatory variables plus an error term:

$$Y_j = x_{j1} * \beta_{1j} + \dots + x_{jl} * \beta_l + \dots + x_{jL} * \beta_L + \epsilon_j$$

where β is an unknown parameter that represents the relative contribution of each of the L explanatory variables. Estimation of β is achieved using the least squares method that will find the ‘best fit’ of the data to the model. We can now identify a regionally specific effect of stimulation expressed as a difference between parameter estimates for separate explanatory variables. In fMRI explanatory variables are often named conditions. The regional effect due to a first condition x_{j1} relative to a second condition x_{j2} , is evaluated using the linear contrast c with $c_1 = 1$ and $c_2 = -1$. In each voxel the statistical variable

$$t = \frac{c_1\beta_1 + c_2\beta_2}{\sqrt{\epsilon^2}}$$

(with β the estimated parameters and ϵ^2 the estimated standard error) is calculated resulting in a t-map for this contrast. In the study of fingersomatotopy, only one condition was evaluated using the linear contrast $c = 1$. The second step of the analysis comprises the application to the map of a threshold value for t , above which ‘unlikely’ values are interpreted as regional activation.

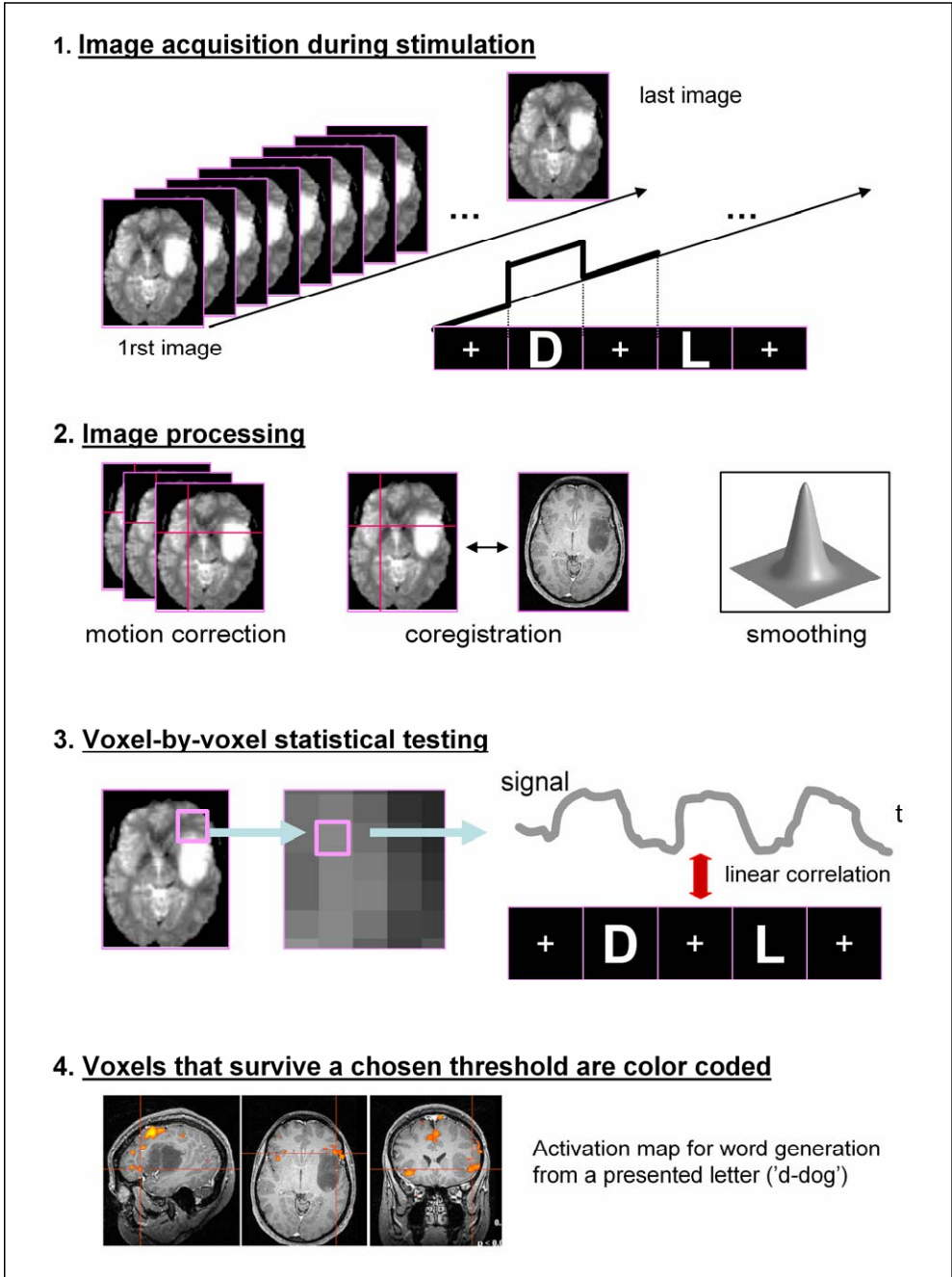


Fig 1: Subsequent steps in an fMRI-study. In this example, linear correlation is used for statistical analysis.

In linear correlation a model of the hemodynamic response is matched to the MRI signal intensity time series [25]. The correlation coefficient r is used to answer the question whether a change in the stimulus over time is associated in a linear fashion with a change in the measured signal in each voxel over time. The correlation coefficient r is calculated as:

$$r = \frac{\sum (X_i - \bar{X})(Y_i - \bar{Y})}{\sqrt{\sum (X_i - \bar{X})^2 \sum (Y_i - \bar{Y})^2}}$$

where X_i is the signal intensity in a given voxel in each of the image volumes, \bar{X} is the mean signal intensity in that voxel over time, Y_i is the reference function over time and \bar{Y} is the mean reference function. A value of $r = 1.0$ or $r = -1.0$ suggests the strongest linear relationship between the two variables.

The resulting t- or r-maps, named ‘activation maps’ below, will display the areas of the brain with significant signal change during stimulation. The activation can be overlaid on either an EPI-image or on high resolution anatomical images. A summary of the subsequent steps in an fMRI study is presented in Figure 1.

b. DTI

Physiological background:

While conventional MR primarily images morphological tissue structures using the contrast obtained by differences in proton density and relaxation times, sequences can also be sensitized to measure the diffusion properties of tissue water. In a free medium, water molecules constantly move and collide randomly with one another, a phenomenon called Brownian motion. In brain tissue, cell membranes and large molecules limit the Brownian motion with the geometrical and physical properties of the tissue determining the rate and preferable diffusion direction [26, 27]. We can thus infer the microstructure of tissue by measuring the water self-diffusion. For example axons in parallel bundles and their myelin sheaths facilitate motion along their main direction where the diffusion is three to six times faster than in the perpendicular direction [28, 29].

Imaging technique and data-analysis:

Sequences sensitized to diffusion usually consist of an echo-planar imaging sequence that includes two strong encoding gradients as first described by Stejskal-Tanner [30]. These gradients which are balanced with respect to stationary protons, induce a diffusion-dependent phase dispersion resulting in a signal loss in areas with higher diffusion. The diffusion sensitivity of the pulse sequence is expressed as the b-value in units s/m^2 and is primarily related to the duration and strength of the diffusion encoding gradient pulses. Measurements including at least two b-values (for example, $b = 0 s/mm^2$ and $b = 1000 s/mm^2$) allow for plotting the logarithmic signal intensity (SI) versus the b-value for a region-of-interest (ROI) or a volume element (voxel) [26]. The slope of this curve is referred to as the apparent diffusion coefficient (ADC) that can be calculated for each voxel. It should be noted that in this

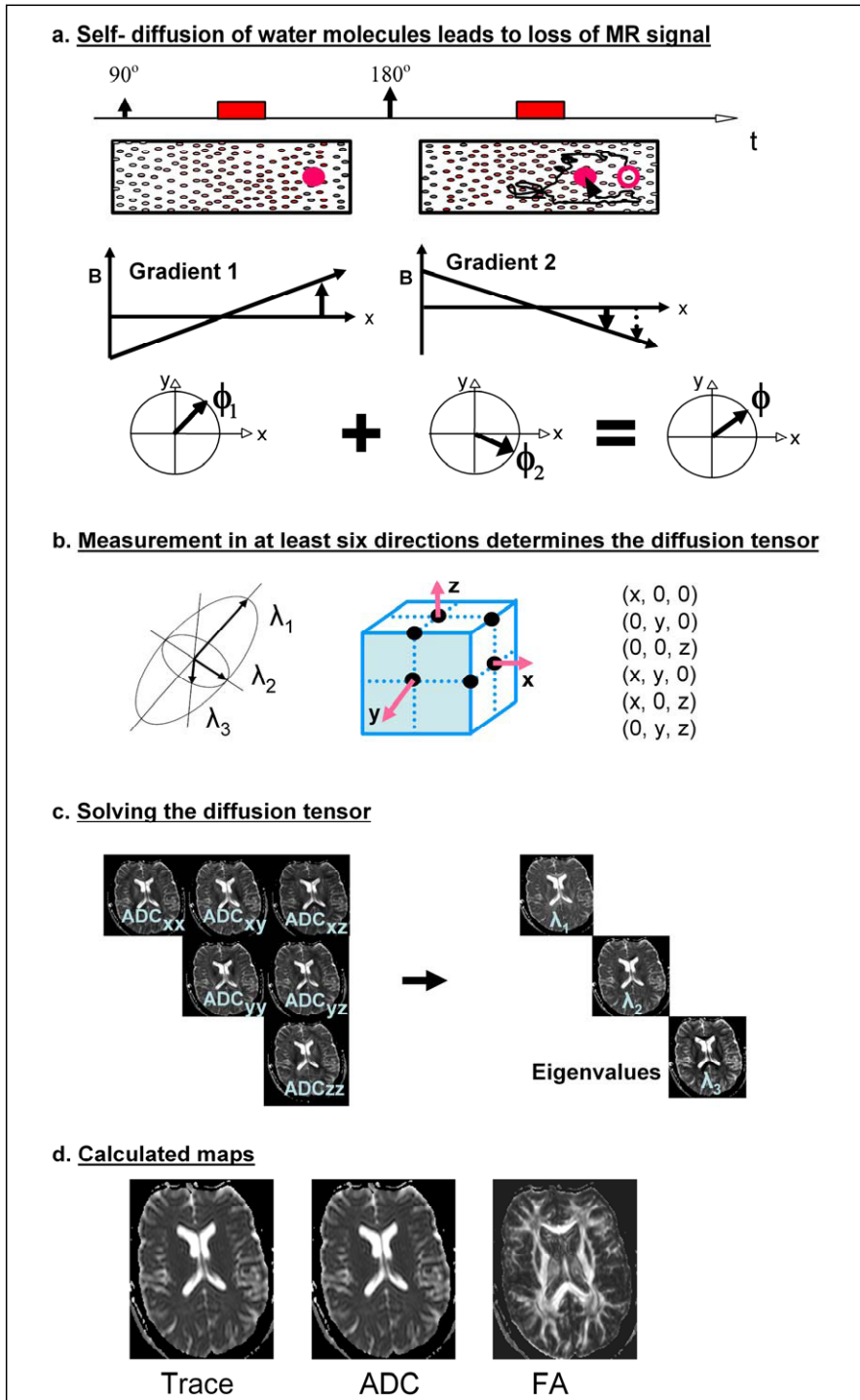


Fig 2: Diffusion Tensor Imaging, (a) showing the principle of diffusion weighted measurements, comprising the application of two gradients balanced with respect to stationary spins and inducing

a phase dispersion for moving spins; (b) determination of the tensor by measurement of the diffusion in six non-colinear directions that describe a Cartesian 3 D coordinate system and the 3 angles that define the orientation of the diffusion in the voxel; (c) solving the 3 x 3 tensor matrix and calculation of parameters; (d) brain maps of Trace, ADC and FA.

diffusion weighted imaging (DWI) as used in the clinical setting e. g. to diagnose stroke or classify brain tumors [31, 32, 33].

In DTI, diffusion weighted measurements are performed in at least six non-colinear directions, resulting in ADC values in six (or more) diffusion encoding directions for each voxel [34, 35]. The ADC analysis calculated from these multiple directions gives the diffusion tensor (D), a 3 x 3 matrix, in each voxel. The diffusion tensor is then solved and the eigenvalues of the tensor are determined. According to the tensor model where the diffusion is described by a sphere or ellipsoid, the eigenvalues reflect the magnitude of the diffusion along the three principal axes of the sphere or ellipsoid [29]. Furthermore, the preferential diffusion direction is given by the largest eigenvalue λ_1 . Strictly speaking, the trace of the diffusion tensor is defined as the sum of the three eigenvalues, however in practise the trace denotes the mean of the three eigenvalues. The mean ADC in a voxel is often a good approximation of the trace. In addition, the fractional anisotropy (FA) index can be determined as:

$$FA = \sqrt{\frac{3}{2}} \frac{\sqrt{\frac{1}{3}((\lambda_1 - \lambda_2)^2 + (\lambda_2 - \lambda_3)^2 + (\lambda_3 - \lambda_1)^2)}}{\sqrt{\lambda_1^2 + \lambda_2^2 + \lambda_3^2}} = \sqrt{\frac{3}{2}} \frac{\sqrt{3Var(\lambda)}}{\sqrt{Tr(\bar{D}^2)}}$$

where $\lambda_1, \lambda_2, \lambda_3$ are the eigenvalues and $Var(\lambda)$ is the variance of the eigenvalues [34]. The FA estimates the degree of anisotropy, i.e. the degree to which water molecules move in one predominant orientation. If diffusion is unconstrained (i.e. isotropic), FA is close to zero; if diffusion has one primary orientation (i.e. is anisotropic), FA approaches 1 [36]. Diffusion calculations are generally carried out on a voxel-by-voxel basis, resulting in Trace (mean ADC)- and FA-maps of the brain. A summary of the principle of diffusion weighted measurements and calculation of the diffusion parameters is presented in Figure 2.

c. Intracranial tumors:

According to the World Health Organisation (WHO) classification of nervous system tumors, intracranial tumors comprise primary tumors derived from normal cellular constituents or from embryologically misplaced tissues and secondary tumors derived from extracranial primary sites that metastasize to the central nervous system [37]. The two largest subgroups of primary tumors are (1) neuroepithelial tumors, in turn subdivided into glial tumors (so called gliomas), neuronal and non-glial tumors and (2) meningeal tumors, including meningiomas. Gliomas are named according to their supposed cell origin. The two most common types of glioma, astrocytic and oligodendroglial tumors, can both be graded according to their degree of malignancy, astrocytomas in four grades with glioblastoma multiforme being the most malignant,

and oligodendrogliomas in two grades. Gliomas grade III and IV, anaplastic astrocytoma and glioblastoma, respectively, account for approximately 38% of primary brain tumors [38]. Tumors with a low grade of malignancy have an intrinsic tendency for malignant progression during the course of the disease, so that glioblastoma multiforme can either arise de novo or progress from a tumor with a lower degree of malignancy [39]. Among the primary intracranial tumors of mesenchymal origin, meningiomas are the most common and account for approximately 27%. Meningiomas are typically well-circumscribed slow-growing tumors, most often with benign histology. Metastases have been reported to occur in 20% to 40% of patients with systemic cancer [40]. They may comprise roughly one third of all intracranial tumors and occur in the skull and dura, leptomeninges and brain parenchyma.

d. The role of MRI in the workup of patients with intracranial tumors:

Although there is no specific symptom of intracranial tumors, slowly progressive focal neurological signs as well as signs of elevated intracranial pressure, should raise suspicion of an intracranial tumor. In addition, a sudden onset of symptoms, such as an epileptic seizure or sudden intracranial hypertension due to bleeding within the tumor, brain swelling or acute hydrocephalus, may occur [38]. Any suspicion of a brain tumor will lead to imaging, with conventional MRI before and after administration of intravenous contrast medium being the test of choice [41]. Some imaging features are characteristic of a certain type of intracranial tumor, for example an extra-axial homogeneously enhancing mass lesion with dural extension will suggest meningioma as the tentative diagnosis [42]. However, imaging findings may be non-specific and the definitive diagnosis is based on histological examination of tumor samples obtained by means of biopsy or surgery. Surgical treatment of low grade gliomas is still under debate, however evidence that more extensive surgery may have a positive effect on outcome is growing [43, 44]. Surgery for high grade glioma provides palliative survival benefit [45], while the role of adjuvant therapies still is under discussion [46]. Meningiomas are often treated by total resection [47]. Resection of metastases may extend survival in properly selected patients [48].

MRI is helpful for the neurosurgeon by providing information about the spatial relationship between the tumor and important brain functions and the extent of tumor growth.

Functional MRI localizes hemodynamic changes in areas of neuronal activity using the blood oxygenation level dependent (BOLD) contrast and has been used extensively to study the organization of cerebral functions, especially cognition, in the normal brain [49]. Clinical fMRI is challenging because paradigms must be adapted to the pathology and mental state of the patient and results may be difficult to interpret due to abundant motion artifacts [76]. Despite these difficulties, fMRI may replace intraoperative cortical stimulation (ICS), the ‘gold standard’ for localization of brain functions. Several studies have demonstrated satisfactory correlation between the site of response to ICS and the area of activation obtained with preoperative fMRI [50-60]. Contrary to ICS, fMRI is non-invasive and can be carried

out preoperatively. However, there are some shortcomings of fMRI that must be kept in mind. fMRI maps an indirect measurement of neuronal activity, namely the hemodynamic response. Coupling of neural activity to BOLD signal may not be constant in the brain or between subjects and decreases in blood flow and oxygen delivery have been reported in the aging population [61]. In addition, fMRI activation is often present in a number of areas that correlate with, but are not necessary for a behavioral task. For example, the cingulate gyrus exhibits activation in language tasks [62], but damage to this structure does not affect speech production to as dramatically as damage to Broca's area. ICS, on the contrary, will reversibly disrupt the function and the effect this has on the patients' language performance is observed, thereby directly assessing the necessity of an area for language. The pathological hallmark of a glioma is that of a highly infiltrative neoplasm. The tumor extent in high and low grade gliomas tends to be underestimated in conventional MR imaging when compared to histopathology [63]. In high grade gliomas, tumor cells typically extend microscopically several centimetres away from the area with signal changes [64]. DTI has been proposed as an alternative to conventional MR imaging for differentiation of signal abnormalities on conventional T2 weighted images between pure edema and tumor-infiltrated edema.

Background of the thesis

Fingersomatotomy in area 3 b of the primary sensory area (Paper 1)

A prerequisite for fMRI to guide safe maximisation of tumor resection is that its spatial resolution is adequate for identifying functional areas. Ever since the BOLD-effect was described, attempts have been made to produce activation maps at increasingly higher spatial resolution. For example, the ocular dominance columns, the functional modules of the visual cortex that are 0.8 -1 mm wide and 20 mm deep, have been mapped using 4 T with a resolution of 0.547 x 0.547 mm [65]. For clinical purposes, the preferred approach has been to identify the somatotopical representations of the body parts in the primary motor (M1) and sensory (S1) cortex that stretch along the pre- and postcentral gyrus. In agreement with the classic homunculus, movement of the hand elicited activation in a digitation of the precentral gyrus, movement of the lips in the lower portion of the gyrus inferior and lateral to the hand area and of the foot at the superior termination of the gyrus near the vertex [54]. It might be of interest to study the representation of body parts smaller than lips, hands and feet. Considering the accurate anatomical definition of the hand area on conventional MR images [66], investigation of fingersomatotomy is an option. The hand representation in the primary sensory cortex (S1) and its subdivisions (areas 3a, 3b, 1 and 2) is somatotopically organised along the central sulcus with the thumb located laterally, anteriorly and inferiorly to the little finger [67]. Area 3b contains neurons that are predominantly responsive to stimulation of cutaneous receptors and possess discrete receptive fields with a homuncular organisation that may be particularly distinct [68]. Previous studies on fingersomatotomy in the hand area of the primary sensory cortex (S1) using functional Magnetic Resonance Imaging (fMRI) have yielded varying results. Gelnar et al. failed to show somatotopy in S1 in response to stimulation of the first, second and fifth finger [69]. Maldjian et al. demonstrated somatotopy in three out of five subjects by stimulating all fingers [70]. Kurth et al., using electrical stimulation of two fingers, found somatotopically arranged activation in five out of twenty subjects [71]. In a follow-up study the same authors reported a general somatotopy without specification [72]. The methods used in these three studies varied considerably with regard to field strength, number of subjects and anatomical considerations. Maldjian et al. used the highest field strength, 4 Tesla (T), while both Kurth et al. and Gelnar et al. used 1.5 T [69-72]. However, Maldjian et al. included a small number of subjects (five) and did not contribute activations to any area in S1 [70]. In the present study we readdressed the issue of somatotopy in the hand area as assessed with fMRI. We aimed at optimising our results by including a large number of subjects (twenty), by focussing on area 3 b, where homuncular organisation expectedly is most distinct, and by performing fMRI at 3 T.

fMRI for preoperative evaluation of intracranial tumors (Paper 2)

The use of fMRI for preoperative evaluation of patients with intracranial tumors is challenging in a number of aspects. Firstly, it must be possible to have the task

paradigms performed by patients who may have functional deficits due to the target lesions adjacent to functional areas. The most commonly mapped functions are motor control, touch and language. Sensory tasks involve presentation of cutaneous stimuli: an assistant outside the scanner delivers rubbing of the hand or foot at 1 Hz. Motor tasks involve active repetitive movements of the appropriate body part (tongue, hand or foot). In paretic patients, passive movement can be used alternatively: movement of the contralateral, healthy hand will then elicit activation in the ipsilateral, affected cortex [73]. Language testing generally involves a verb generation task, also named verbal fluency task, that requires both language comprehension and expression, for example generating words from a presented letter (d - dog) [74]. In the clinical situation simple paradigms with word generation alternated with fixation are often used. In the worst case scenario, where the patient is unable to produce language but can understand it, the paradigm might consist of listening to a text and fixation. Secondly, the task paradigms should elicit robust activation on the subject level resulting in activation maps that allow for unequivocal identification of important functional areas. Motor and sensory stimulation with fingertapping and rubbing of the hand, respectively, may fulfil these requirements provided no motor and sensory deficits are present [75]. Since movement artefacts during motor stimulation can cause major problems when activation maps are evaluated, instruction of the patient, head fixation and supervision by an assistant outside the scanner are critical [76]. Artefacts associated with language stimulation using silent word generation as opposed to overt word generation have been shown to be less frequent because of decreased head and neck movements [77, 78]. One disadvantage of silent word generation is the inability to monitor subject performance of the task. This disadvantage can be corrected for by involving the use of a response box with the patient or subject pressing one of several buttons depending on the task. Thirdly, the therapeutic relevance of preoperative fMRI as regards its ability to estimate the risk of surgical treatment must be evaluated. Lee et al reviewed the medical records of 46 patients who had undergone fMRI and determined the extent and nature of influence on patient management with special attention to 1) the use of fMRI for assessing the risk associated with, and hence feasibility of the proposed surgery (70 %), 2) its use for guiding placement of the bone flap (43 %) and 3) its use for determining the need for ICS (52 %) [79]. Haberg et al reported the use of fMRI activation maps for preoperative planning in 75 % of cases by the neurosurgeons at their institution [80]. The same authors found that the risk for postoperative function loss was significantly reduced when the distance between tumor periphery and BOLD activation was 10 mm or more, well in accordance with previous studies comparing fMRI and ICS [52] and evaluating ICS [81]. Bearing this mind, we started a prospective study on preoperative fMRI as a tool for localising brain functions at the time when a 3 T MR scanner became available for clinical purposes. Twenty patients were studied using simple paradigms applicable in clinical routine. We rated the diagnostic quality of the activation maps, taking into consideration the achievement of fMRI and the presence of artefacts. Finally, we report on the influence of fMRI on neurosurgical decision-making regarding operability, surgical approach and extent of the resection.

The effect of glioma resection on fMRI activation (Paper 3)

High grade gliomas may show rapid progression even after primary surgery and patients may be operated upon several times during the course of their disease. Preoperative fMRI may thus be performed before and after glioma resection and even after a second or third resection. The assessment of activation maps from postoperative fMRI may be hampered by alterations in the hemodynamic response in the vicinity of glial tumors where pathologic vessels may interfere with neurovascular coupling. Hitherto results are inconsistent and include reports on lower numbers of voxels activated during motor stimulation near gliomas than in the vicinity of nonglial tumors [82, 83]. Comparisons between gliomas and healthy controls resulted in a lack of change during language stimulation [84] and increase during PET and language stimulation in one patient with a high grade glioma [85]. On the other hand, the test-retest reproducibility of the spatial extent of fMRI activation is low in healthy controls. For example, the ratio of the number of voxels that is active in both of two iterations of a task to the number active in either iteration, is 1.0 in case of perfect correlation, but was 0.57 for motor and sensory stimulation [86] and 0.24 for language stimulation using a verb generation task [87]. Therefore, we wanted to determine the spatial extent of motor, sensory and language activation pre- and postoperatively in glioma patients and compare the results to those obtained from repeated examinations in controls.

DTI for characterisation of tumor edema (Paper 4)

Studies on the use of DTI for characterisation of T2-signal changes surrounding high grade gliomas, have compared measurements from high grade gliomas with those from meningiomas and sometimes metastases, under the assumption that T2-signal changes surrounding meningiomas and metastases consist of pure edema [88-101]. The results are conflicting: one study found a difference between high grade gliomas and meningiomas in peritumoral ADC and FA [88]; a second study found a difference between tumor types in peritumoral ADC, but not in peritumoral FA [95]; and a third study found no difference between tumor types in peritumoral ADC or FA [98]. The fact that measurements were compared regardless of the location of the tumor may be a drawback in these studies. ADC and especially FA are known to vary substantially within the brain.

We compared measurements from high grade gliomas with those from meningiomas and metastases, under the assumption that T2-signal changes surrounding meningiomas and metastases consist of pure edema. Because ADC and especially FA are known to vary substantially within the brain, we calculated lesion-to-brain ratios of ADC and FA from measurements in brain tissue with peritumoral signal changes and the adjacent normal appearing white matter (NAWM) and in the corresponding anatomical site in the contralateral healthy hemisphere.

Material and Methods

Fingersomatotopy in area 3 b of the primary sensory area (Paper 1)

Twenty healthy, self-reportedly right-handed volunteers (6 male and 14 female, age 21–43 years, mean 29.4 years) were included in the study.

Tactile stimulation consisted of brushing the glabrous skin of the two distal phalanges of each finger continuously forwards and backwards with a tooth brush. The frequency was 1 Hz; no forced pressure was exerted.

Functional echo-planar image volumes of the whole brain (number of slices = 49, thickness = 3 mm, voxel size = $3 \times 3 \times 3 \text{ mm}^3$, no gap) sensitized to the BOLD-effect (echo time = 30 ms) were acquired using a 3 T head scanner (Siemens Allegra) with a quadrature birdcage coil. A session included 92 functional volumes with a temporal resolution of 3 seconds. The first two volumes in each session were discarded to allow for initial T1-equilibrium effects. A heavily T2-weighted FLAIR-sequence (TR=9000 ms/TE=81 ms/TI=2500 ms) was performed to rule out pathology and a T1 weighted 3 D magnetization prepared gradient echo sequence (MPRAGE, TR=2500 ms/TE 4.38 ms, voxel size $1 \times 1 \times 1 \text{ mm}$) was acquired for coregistration.

Image processing and analysis were carried out using the SPM99 software package [19]. All functional images were resliced to voxel size $1.5 \times 1.5 \times 1.5 \text{ mm}^3$ and then realigned to the first image and coregistered to the T1-weighted image volume. All data were spatially smoothed using an isotropic 4 mm, full-width, half-maximum Gaussian kernel. A high pass filter (cut off frequency 0.008 Hz) was applied to eliminate low frequency signal fluctuations.

Task specific effects were estimated using the general linear model (GLM) as implemented in SPM. The spatial coordinates of the peak activation voxel in area 3b were determined using an operational definition of area 3 b as the anterior wall of the postcentral gyrus [102, 103]. The spatial coordinates of the peak voxel for the thumb (D1) were defined as being at origo (0, 0, 0) in a 3D Cartesian coordinate system. Somatotopy was assessed by determining the average distances for the whole group from each finger to the thumb. Euclidian distances between fingers as well as from each finger to the thumb (D1) were calculated. Non parametric statistics were used. Each finger's distance to the first finger was compared to that of the directly neighbouring fingers using the Wilcoxon matched pairs test with a significance level of $p < 0.05$. The Euclidian distances to the first finger were compared for each finger using the Wilcoxon matched pairs test with a significance level of $p < 0.05$.

fMRI for preoperative evaluation of intracranial tumors (Paper 2)

Twenty patients (13 male and 7 female, mean age 42.1 years, range 27-60 years) considered for neurosurgical treatment of an intracranial tumor were prospectively examined with fMRI in addition to previous morphological MRI. A putative relationship (distance 2 cm or less) between the tumor and the primary sensorimotor or language cortex on conventional MRI was required for inclusion in the study. Histological diagnosis was available for eighteen patients. In two patients the probable diagnosis of low grade glioma was based on imaging findings.

Motor, sensory and language stimulation was performed. Motor stimulation consisted of finger tapping, sensory stimulation was performed by brushing the right hand with a rough sponge. Language stimulation included a verbal fluency task (generation of words beginning with a predefined letter) and rhyming. Each paradigm consisted of three activation blocks and four baseline blocks of 30 s each. The baseline task consisted of viewing a cross.

Functional echo-planar image volumes of the whole brain (number of slices = 36, thickness = 3 mm, voxel size = $3 \times 3 \times 3 \text{ mm}^3$, gap = 0.9 mm) sensitized to the BOLD-effect (echo time = 30 ms) were acquired using a 3 T head scanner (Siemens Allegra) with a quadrature birdcage coil. A session included 72 functional volumes with a temporal resolution of 3 seconds; the first two volumes were discarded to allow for initial T1-equilibrium effects. A heavily T2-weighted FLAIR-sequence (TR=9000 ms/TE=81 ms/TI=2500 ms) was performed to visualise non-enhancing tumor and edema. For the purpose of coregistration a T1 weighted 3 D magnetization prepared gradient echo sequence (MPRAGE, TR=2500 ms/TE 4.38 ms, voxel size $1 \times 1 \times 1 \text{ mm}$) was acquired after injection of a gadolinium based contrast agent (0.1 mmol/kg body weight).

Raw data were corrected for head motion using an algorithm supplied by the manufacturer of the MRI scanner [104]. Slice timing, linear trend removal and high pass filtering were performed using commercially available software (Brain Voyager 4.9, BrainInnovation BV, Maastricht, The Netherlands) [20]. Coregistration with the high resolution anatomical sequence was performed. Significantly activated pixels were identified by cross-correlation with the use of a reference function reflecting the activation, shifted by one image volume to account for hemodynamic latencies [25]. Voxels surviving a threshold of $r_{\text{max}} > 0.4$ in clusters of 3 or more were accepted for further analysis and displayed on anatomical 3D-data sets.

Data analysis focused on paradigm effectiveness, quality of the activation maps and neurosurgical decision making. The effectiveness of each paradigm was determined as the percentage of patients in whom activation in the functional area of interest was found relative to the number in whom the paradigm was performed. The combined effectiveness of motor and sensory stimulation and of the two language paradigms was determined using a logical 'or' decision. The quality of the activation maps was assessed subsequent to establishing a working threshold that was generated by increasing the threshold in steps of 0.02 until activation could be separated from motion artefacts and noise. The presence of susceptibility artefacts on EPI-images was noted. The quality of the activation maps was rated on a scale from 1 to 3 where 3 represents high diagnostic quality allowing for unequivocal identification of important functional areas, 2 indicated quality that was adequate for diagnostic purposes, but inferior to 3 due to motion or other artefacts and 1 was applied in cases where activation was insufficient for localisation purposes due to either unsuccessful stimulation or failure to separate activation from motion artefacts. The distance between the tumor and the functional area of interest was calculated as the shortest Euclidian distance between the margin of the activated area at the working threshold and the tumor margin as assessed from 3D T1-weighted and FLAIR-images; the value was approximated to the nearest 0.5 cm. Activation maps, clinical symptoms,

tentative histological diagnosis, tumor location and its relationship to functional areas were reviewed together with the neurosurgeon. Operability (a), surgical approach (b), and the extent of resection (c) were assessed and the influence of fMRI on a, b and c was reported by the neurosurgeon. Non parametric statistics were used and analyses were performed using Friedmans test, Wilcoxon's matched pairs test and McNemars test for correlated proportions; $p < 0.05$ was considered significant.

The effect of glioma resection on fMRI activation (Paper 3)

Six patients with low or high grade gliomas in the left hemisphere in putative close proximity (distance 2 cm or less) to primary sensorimotor or language cortices were included in the study. All patients were recruited from the material of twenty consecutive patients studied in Paper 2 and underwent fMRI preoperatively as well as early (within 1 week) and late (after 2 months) postoperatively. Six neurologically healthy controls underwent fMRI twice within one week and on a third occasion two months later.

The experimental protocol and imaging parameters were similar used to those in Paper 2. Processing of functional volumes prior to analysis differed from that in Paper 2, in that coregistration with anatomical images was not performed.

Data analysis included calculation of the number of activated voxels in regions of interest (ROI) drawn in both hemispheres in the hand area in the primary motor and sensory cortex and the left and right frontal language areas located in the inferior and middle frontal gyri. For all paradigms the laterality index (LI) was determined as $LI = (L-R)/(L+R)$, where L and R represent the number of activated voxels in the left and right frontal lobe, respectively [105].

Statistical analyses were performed using Wilcoxon's matched pairs test for within-group comparisons and Mann Whitney U test for between-group comparisons; $p < 0.05$ was considered significant.

DTI for characterisation of tumor edema (Paper 4)

Thirty patients were included: 18 WHO grade III or IV gliomas, seven meningiomas and five metastatic lesions. All gliomas, four of the meningiomas and three metastatic lesions were biopsy-proven. In two of the meningiomas diagnosis was based on typical imaging findings. In one patient with metastases from breast cancer, diagnosis was based on imaging findings and clinical history; in a patient with metastases from carcinoma of the ureter, the diagnosis was provided by cytology from cerebrospinal fluid.

Imaging was performed with a Siemens Allegra head scanner in twenty-four patients and with a Philips Intera scanner in six patients (three gliomas, two meningiomas and one metastasis). The imaging protocol included conventional T1-weighted spin echo images before and after contrast injection (Allegra:TR/TE = 600 ms/11 ms; Intera:TR/TE=500 ms/10 ms), turbo spin echo T2-weighted images (Allegra:TR/TE = 4000 ms/23 ms; Intera:TR/TE=3000/80) and diffusion sensitized sequences for diffusion tensor imaging (DTI). The conventional sequences contained 23 slices of 5 mm thickness and 0.5 to 1.5 mm interslice gap. The gadolinium based contrast agent was injected after DTI had been performed.

On the Allegra, the DTI image data set was acquired by means of a sequence with diffusion encoding performed in twelve non-colinear gradient directions, using three b-values (0, 300 and 1000 s/mm²). On the Intera, the DTI data set was acquired by means of a single shot-EPI diffusion weighted sequence provided by the manufacturer with diffusion encoding performed in fifteen non-colinear gradient directions, using two b-values (0, 800 s/mm²). Four averages of b=800 s/mm² were acquired using SENSE with reduction factor 2.5.

ADC and FA values were determined using 20-30 mm² large ROIs on the ADC- and FA-maps in the peritumoral areas with T2-signal changes as well as the adjacent NAWM in both hemispheres. Lesion-to-brain ratios were calculated by dividing the value in either the peritumoral signal changes or the adjacent NAWM with the value in the normal brain at the same anatomical site contralateral to the tumor.

Values and lesion-to-brain ratios of ADC and FA in peritumoral areas with T2-signal changes and in adjacent NAWM were compared between gliomas, meningiomas and metastases using the Kruskal Wallis ANOVA by ranks test and further analyzed with the Mann Whitney U test. The level of significance was set at $P < 0.05$.

Results

The following is a summary of our results. For more detailed information, the reader is referred to Papers I-IV.

The spatial resolution of clinical fMRI (Paper 1)

Significant activation observed for all five fingers in area 3b present of seventeen subjects was available for analysis. A somatotopic organisation with the representation of the thumb located laterally to the little finger was present in 16 out of 17 subjects, with the thumb located anteriorly to the little finger in 14 out of 17 subjects and with the thumb located inferiorly to that of the little finger in 16 out of 17 subjects. Group averages of the distances from D2 to D1 (D2-D1), D3 to D1 (D3-D1), D4 to D1 (D4-D1) and D5 to D1 (D5-D1) indicate a strict somatotopy with the distance to D1 increasing for every finger in each of the three directions (Figure 3). The Euclidian distance from D1 to D2 was 10.6 mm (SEM \pm 1.5). The distance from D2 to D3 was 5.5 mm (\pm 0.9), from D3 to D4 7.4 mm (\pm 1.1) and from D4 to D5 6.8 mm (\pm 1.2), resulting in an average for D2-D3, D3-D4 and D4-D5 of 6.6 mm. The spatial extension of the representation of the hand in area 3b, defined as the Euclidian distance between D1 and D5 was 17.2 mm (\pm 2.0 mm).

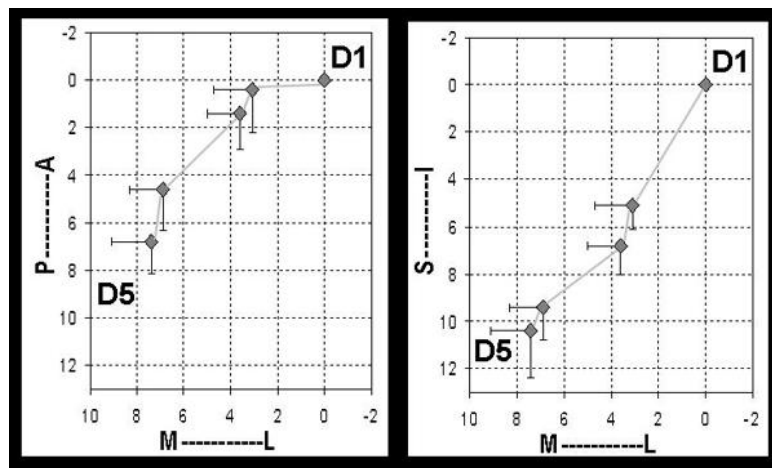


Figure 3 : Distance to the thumb (D1) of each finger (mm), mean (diamonds) and SEM (errorbars), P=posterior, A= anterior, S=superior, I=inferior, M=medial, L=lateral

fMRI for preoperative evaluation of intracranial tumors (Paper 2)

The main functional area of interest for the neurosurgeon was the central sulcus in eight patients and the frontal or temporal language areas in twelve patients.

Paradigm effectiveness: The contralateral M1 was identified in 18 out of 20 patients and the contralateral S1 in 18 out of 19 patients; this result was similar for the combination of paradigms according to the logical 'or' decision. Word generation

and rhyming were equally effective at activating the left and right IFG as well as the left and right STG (McNemars test, $p=1.0$, $p=0.22$, $p=0.24$ and $p=0.75$).

Quality assessment: The median quality of the activation maps rated 3 (high) on an ordinal scale for all paradigms (Figure 4). In 19 out of 20 patients three of four paradigms generated activation maps rated as 2 or 3, making the fMRI study as a whole successful. In patient 17, no activation maps of diagnostic quality were obtained for any paradigm. Due to severe motion artefacts no working threshold $cwas$ obtained in this patient. Susceptibility artefacts observed on EPI-images in nine patients were caused by drill holes in seven cases and blood within a tumor cyst in two cases. Such artefacts were located within 2 cm of the functional area in three cases (patient 11, 13 and 16).

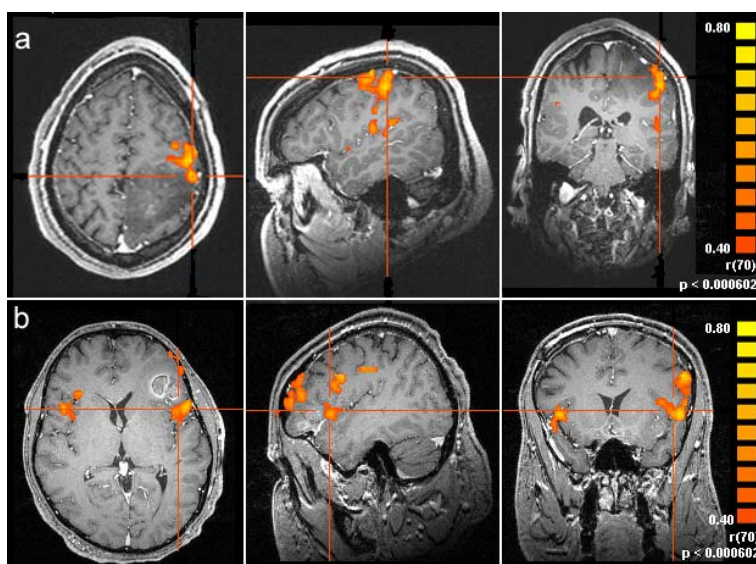


Figure 4 : Spatial relationship between tumor and fMRI activation in **(a)** the sensorimotor area and **(b)** Broca's area in the left IFG; axial, sagittal and coronal views. **(a)** High quality activation map from sensory stimulation of the right hand in patient 12 with a biopsy-proven low grade astrocytoma in the left superior parietal lobule. Activation in the contralateral, left sensory motor cortex anterior to the tumor at a distance of 0 cm is marked by crosshairs. fMRI aided in deciding not to resect the tumor.

(b) : High quality activation map from language stimulation (word generation) in patient 2 with a melanoma metastasis in the frontal operculum in the language dominant hemisphere. Activation is present bilaterally in the inferior frontal gyrus, predominantly in the left that is marked by crosshairs. The distance between the tumor and activation in Broca's area is 0 cm. fMRI facilitated the decision-making regarding the decision to operate and the extent of the resection.

Relation between tumor and activation: For tumors close to the sensorimotor cortex, the median distance to the activation was 0.5 cm (range 0-2 cm). For tumors near language areas, the median distance to the activation was 1 cm (range 0-2 cm). Mass

effect was present in fifteen patients leading to sulcal effacement and subsequent difficulties in the interpretation of the anatomy from morphological images in twelve. **Neurosurgical decision-making:** Seventeen patients were accepted for tumor resection, aiming at radical excision in patients with putative metastasis and meningioma. In patients with primary brain tumors, resection aimed at debulking of the tumor mass. fMRI influenced the surgical approach in thirteen patients and the extent of the resection in twelve. Twelve patients were operated upon within three months after fMRI was performed, with a transient postoperative paresis contralateral to the tumor occurring in two of these.

The effect of glioma resection on fMRI activation (Paper 3)

A comparison of the data from the three time points for examination failed to reveal a longitudinal difference in LIs for any paradigm between the groups (Figure 5 a, b, c and d). The median LIs for motor and sensory stimulation did not differ between patients and controls (Table 3). Since the LIs for verbal fluency and rhyming were larger than 0 in all volunteers, but lower than 0 in patient 5 for both tasks and in patient 3 for rhyming, no between group comparison was done for language stimulation.

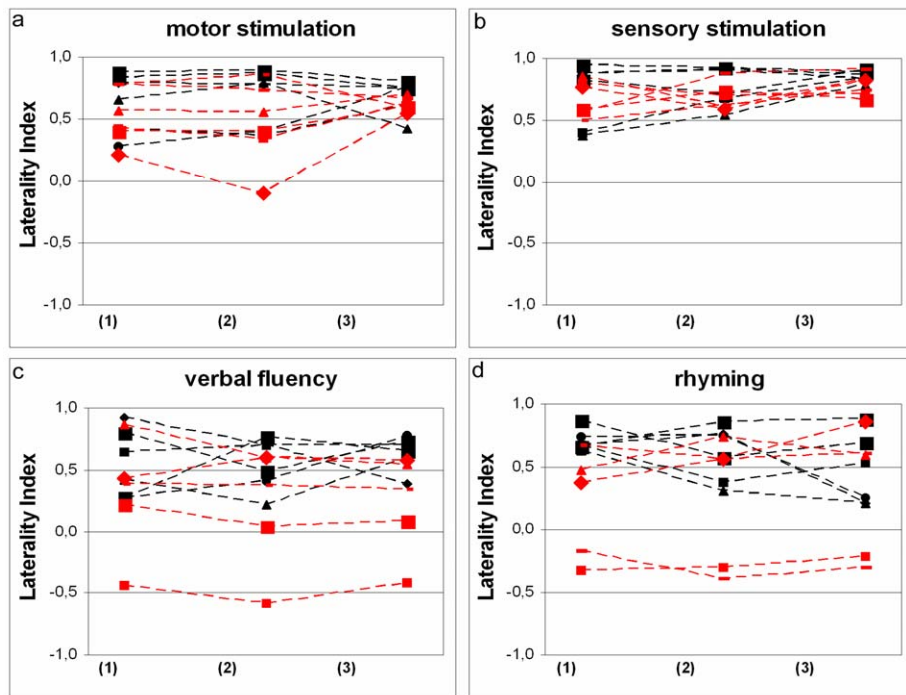


Figure 5 a, b, c and d: Laterality indices for motor (a) and sensory stimulation (b), for the verbal fluency task (c) and for rhyming (d) from each patient and control preoperatively (1), early (2) and late postoperatively (3) and the first (1), second (2) and third (3) examinations; patients are represented by red and controls by black symbols.

DTI for characterisation of tumor edema (Paper 4)

The value of ADC, the lesion-to-brain ratios of ADC, the value of FA and the lesion-to-brain ratio of FA in the peritumoral areas with T2-signal changes did not differ between the three tumor types ($p=0.4014$, $p=0.4027$, $p=0.6144$, $p=0.3408$, Kruskal Wallis ANOVA by ranks). The value of ADC as well as values and lesion-to-brain ratios of FA in the adjacent NAWM did not differ between tumor types ($p=0.7350$, $p=0.2483$ and $p=0.3064$). The lesion-to-brain ratio of ADC in the adjacent NAWM was higher in gliomas than in meningiomas and metastases ($p=0.0041$). However, an overlap of the ranges of this ratio for the three tumor types was observed (Table).

Table: ADC and FA values and lesion-to-brain ratios in peritumoral T2-changes and adjacent NAWM, median (range)

		Gliomas	Meningiomas	Metastases
Peritumoral T2-changes	FA value	0,194 (0,089 - 0,451)	0,163 (0,108 - 0,206)	0,164 (0,108 - 0,195)
	FA ratio	0,423 (0,203 - 0,716)	0,363 (0,256 - 0,417)	0,357 (0,256 - 0,385)
	ADC value ($10^{-3} \text{ mm}^2/\text{s}$)	1,505 (0,887 - 1,976)	1,635 (1,528 - 1,887)	1,527 (1,174 - 1,784)
	ADC ratio	1,885 (1,112 - 2,630)	2,089 (1,820 - 2,430)	1,857 (1,638 - 2,086)
Adjacent NAWM	FA value	0,395 (0,255 - 0,593)	0,389 (0,290 - 0,561)	0,353 (0,279 - 0,561)
	FA ratio	0,928 (0,485 - 1,175)	0,836 (0,763 - 1,109)	0,938 (0,763 - 1,057)
	ADC value ($10^{-3} \text{ mm}^2/\text{s}$)	0,820 (0,713 - 0,937)	0,796 (0,706 - 0,926)	0,815 (0,706 - 0,862)
	ADC ratio	1,059* (0,933 - 1,131)	0,996* (0,948 - 1,019)	1,006* (0,948 - 1,035)

*: $p=0.0041$, Kruskal-Wallis ANOVA for ranks, when tumor types are compared

Discussion

General remarks: fMRI and field strength

The introduction of 3 T MR scanners for use on a broader basis than basic research, including clinical use, was triggered by the interest among neuroscientists in pursuing fMRI studies on cognition at a higher field strength. Increases in spatial resolution, number of activated voxels, t-value in activated voxels and percentage of signal change between activation and rest have been reported in response to increases in field strength from 1.5 T to 3 T or 4T for motor and visual stimulation as well as for a working memory task [19, 106-109]. The advantages of using higher field strengths include increased sensitivity to susceptibility, increased contrast to noise and improved sensitivity and spatial specificity for detection of task-related brain activation. The latter is a result of the observation that the rate of transverse relaxation, $1/T2^*$ or $R2^*$, scales with the square of the external magnetic field for small blood vessels and capillaries, whereas the change is linear for large blood vessels [110, 111]. In one study on motor and visual stimulation, the increase in field strength from 1.5 T to 3 T a gain in the contrast to noise ratio (CNR) of more than 2 in the average activated brain voxel was accompanied by a 1.8 fold increase in the mean z-score in activated brain regions [107]. During a working memory task (two-back task) activation volumes in the frontal and parietal lobes were increased at 3 T as compared to 1.5 T [108]. Activation in several regions has been detected at 3 T but not at 1.5 T [108, 109]. While this thesis does not attempt to offer a direct comparison of fMRI at different field strengths, such comparisons can be found in the literature.

Fingersomatopy in area 3 b of the primary sensory area (Paper 1)

The main result of this paper was that the observation that the strict somatotopic organisation in the primary sensory cortex known from studies using a variety of modalities, was reproduced in the group average. The average activations of the fingers were laid out on the body map, with the thumb located most laterally, anteriorly and inferiorly and the little finger most medially, posteriorly and superiorly and the remaining fingers in between. The distance to the thumb increased for every finger in each of the three directions. In individual subjects the arrangement in the hand representation of the thumb located laterally, anteriorly and inferiorly to the little finger was observed frequently, while the remaining fingers might display the orderly lateral-to-medial, anterior-to-posterior and inferior-to-superior organisation 'D1-D2-D3-D4-D5'. These results suggest that the spatial resolution of fMRI at 3 T in a clinical setting is sufficient to delineate the functional areas of interest as regards preoperative functional mapping. The cortical surface devoted to an individual digit in area 3b is in the order of 0.5 to 1 mm² in the owl monkey [112] and given the difference in brain size between macaques and humans, the expected cortical area devoted to a single fingertip in humans should be about 5 mm². This is well in concordance with our results where the average Euclidian distance from D2 to D3, D3 to D4 and D4 to D5 was 6.6 mm with distances calculated between the peak activated voxels of the fingers. Furthermore, the average extension of the hand

representation in area 3b of 17 mm with a somatotopic arrangement of fingers 1-5 as described above is consistent with results from previous studies using a range of modalities [69-72, 113-115]. For example, by using magnetoencefalography, Hari et al. calculated equivalent current dipoles (ECD) from magnetic field patterns obtained during electrical stimulation of the fingers [113]. ECDs for eight subjects were concentrated to strips of < 2 cm in length with the thumb generally represented more laterally and the fifth finger most medially.

Previous studies on somatotopy in the hand area using functional Magnetic Resonance Imaging (fMRI) have applied different types of sensory stimulation including vibratory stimuli generated with inhouse developed devices [69, 70] and electrical stimulation using ring electrodes [71, 72]. While all these methods are likely to activate neurons in area 3b, they may differ as regards the number of activated voxels. When comparing the effect of electrical stimulation of the median nerve at two different frequencies and of tactile stimulation of the right index finger using a watercolour camel-hair paintbrush, Boakye et al failed to detect a difference in activation volumes between electrical and tactile stimulation [116]. Possible factors influencing results of our study as compared to the works mentioned above may include the number of subjects, the number of fingers studied, the field strength and other imaging parameters as well as anatomical considerations taken into account during data analysis. Due to lack of neuroanatomical landmarks, exact delineation of the cytoarchitectonically defined areas within S1 cannot be achieved in MR images. The operational definition that we used with area 3b being located in the anterior bank of the postcentral gyrus is easily applied in transverse images [102, 103]. However, its application in coronal or sagittal orientation, especially when slice thickness is large, is more challenging. In addition, the well defined landmark of the motor hand knob situated on the precentral gyrus and protruding into the central sulcus, is identified in the transverse plane. Gelnar et al. studied the first, second and fifth fingers in eight subjects without demonstrating somatotopy [69]. In their study eight coronal slices with high in-plane but relatively low through-plane resolution ($1.56 \times 1.56 \times 6 \text{ mm}^3$) were obtained. Maldjian et al. stimulated all fingers in five subjects and found somatotopy in three where the thumb to fifth finger with a lateral to medial, inferior to superior and anterior to posterior relationship [70]. Activated voxels were attributed to S1 without distinguishing between areas within S1. Kurth et al. studied the second and fifth finger and found somatotopically arranged activation patterns area 3b in 5 out of 20 subjects [71]. The same authors reported a general somatotopy without specification in a follow-up study where activation of all fingers in area 3b was found in 7 out of 10 subjects, [72]. However, Kurth et al performed this study at 1.5 T. Our finding of somatotopy with the thumb to fifth finger having a lateral to medial, inferior to superior and anterior to posterior relationship in 16 out of 17 subjects may be due to the use of higher field strength.

fMRI for preoperative evaluation of intracranial tumors (Paper 2)

In this study, the sensorimotor and language areas close to intracranial tumors were identified in 95 % of patients by using fMRI at 3 T. Paradigm effectiveness was 90 % for motor and 95 % for sensory stimulation and ranged from 79 to 95 % for language

stimulation. The median quality of the activation maps was 3 (high) for all paradigms. fMRI contributed to the decision to operate in 9 patients, the surgical approach in 13 patients and the extent of the resection in 12 patients.

Paradigm effectiveness: Our use of multiple paradigms aimed at maximising their effectiveness in localising the sensorimotor cortex and language areas. Finger tapping and passive touch activate the primary motor and sensory cortex, and word generation and rhyming both activate the IFG and STG. The reported increase in paradigm sensitivity associated with multiple paradigms [75, 87] was not confirmed in the present study. However our confidence in assessing activation maps was increased due to the availability of results from two paradigms.

Quality assessment: Evaluation of activation maps in a clinical setting requires a cautious approach. The optimal threshold for a paradigm in a particular patient is never known: increasing the threshold may generate false-negative results and decreasing the threshold certainly generates false positive activation. We opted to define a working threshold for each patient, that was as close as possible to the minimum threshold $r > 0.4$ without including motion artefacts interfering with identification of functional areas. Our median working correlation threshold for all paradigms was 0.44, range 0.40-0.60. For comparison, in a recent study at 1.5 T the mean working threshold was 0.54 with standard deviation ± 0.08 [80]. Our results indicate that clinical fMRI at 3 T might have the advantage of generating high quality activation maps at lower thresholds.

Relation between tumor and activation: The threshold used for the activation maps, influences the distance between the tumor and the functional area. For the purpose of reporting our results, we used the working threshold to measure the distance in multiples of 0.5 cm. We informed the neurosurgeon of the impact of the threshold and the potential lack of activation in primary functional areas as well as of other limitations of fMRI. Due to their sensitivity to magnetic susceptibility changes, EPI images are often associated with distortion, notably in the vicinity of air cavities. The distortion may increase with increased field strength. We determined the distortion in the EPI-images produced by our system by means of a field map [117]. The average displacements were smaller than ± 3 mm (SD < 1 mm) in the sensorimotor cortex and the frontal language area.

Neurosurgical decision-making: Decisions regarding operability, surgical approach and extent of resection were based on the information gathered from clinical history and examination, tentative histological diagnosis and results from fMRI. By providing results preoperatively, fMRI offers a major advantage to the neurosurgeon compared to e.g. ICS [79]. In addition, fMRI results can be correlated with results from other imaging modalities and thereby facilitate preoperative decision-making and planning [118]. The procedure therefore contributes to a well informed and critical discussion with the patient regarding the risks and benefits of surgical intervention.

The effect of glioma resection on fMRI activation (Paper 3)

The main result of our study was the observation that BOLD activations obtained from motor, sensory and language stimulation using pre- and postoperative fMRI in

glioma patients yielded differences in the spatial extent similar to those obtained from repeated examinations in healthy controls. Our findings suggest that longitudinal studies using fMRI can be performed in patients undergoing glioma resection without concerns about negative effects of the decreased tumor volume on the BOLD effect. Gliomas have been reported to influence the BOLD response in different directions during preoperative fMRI. Schreiber et al. found reduced BOLD activation near gliomas and unaffected activation near nonglial tumors during a bilateral motor task [83]. In this work the authors refer to unpublished data from two healthy volunteers examined 11 and 12 times on different days, with a variability of 23 % in the voxel ratio (the ratio of the numbers of voxels activated in the contra- and ipsilateral hemisphere). However, in a comparison between eight controls and six patients with gliomas of various grade, Schlosser failed to detect a difference in the mean voxel z-score and cluster size during language stimulation [84]. Recently Kokkonen et al. sought to further explore the effect of gliomas on the BOLD response by performing fMRI pre- and postoperatively [119]. Seven patients were examined pre- and postoperatively using bilateral motor and auditory stimulation, five underwent fMRI early and late postoperatively. The extent of the fMRI activation, expressed as the voxel ratio, varied at the three time points, with an increase in some patients and a decrease in others.

Longitudinal fMRI studies are known to be associated with low within-subject test-retest reproducibility, an issue that has been addressed mainly in healthy volunteers [86, 87]. Measurement parameters have included the number of overlapping voxels and the distance between centers of mass as calculated from the voxel location in a Cartesian 3 D coordinate system. Postoperative brain displacement precludes the ready use of these parameters for comparative studies pre- and postoperatively. We decided to use the laterality index (LI) that offers the additional advantage of relating activation in one hemisphere to the corresponding activation in the opposite hemisphere. Thus potential global variations in the number of activated voxels are minimized, hence making the LI a suitable parameter for longitudinal studies. The LI is a well-known parameter for determination of hemispheric language dominance [105]. In our study the LIs in motor and sensory stimulation were slightly, although not significantly smaller in patients as compared to controls. This may be attributed to the more abundant motion artefacts in patients [76], leading to an increase of the number of voxels activated bilaterally and to a somewhat lower LI. Alternatively, this may be explained by a reduction of the local activation seen in the vicinity of gliomas.

Titanium fixation clamps were implanted intraoperatively in patients 2, 4 and 6 and were present preoperatively due to biopsy or surgery in patients 1, 3 and 5. This could be a possible source of concern, since these clamps have the disadvantage of extinguishing the MR-signal in their vicinity resulting in a signal void of approximately $1.5 \times 1.5 \times 1.5 \text{ cm}^3$. We are nevertheless confident that we have been successful in accurately identifying the functional areas stimulated and determine the number of activated voxels. In patients 2, 4, and 6 the tumor and the adjacent functional area of interest were located at some distance from the clamps. Patient 1, 3 and 5 had been operated previously and the clamps were reimplanted at the same

location so that the possible error due to signal extinction was similar in the pre- and postoperative study.

DTI for characterisation of tumor edema (Paper 4)

Our main observations were a lack of difference in ADC and FA between high grade gliomas, meningiomas and metastases when values and lesion-to-brain ratios from peritumoral areas with T2-signal changes were compared. This suggests that DTI may not be adequate for differentiating between pure edema and tumor-infiltrated edema in peritumoral areas. In the adjacent NAWM the lesion-to-brain ratio of ADC, was higher in gliomas than in meningiomas and metastases. However, ranges overlapped for the three tumor types, suggesting that such measurement may not be suitable for clinical evaluation.

ADC values range from 0.6 to $1.0 \times 10^{-3} \text{ mm}^2/\text{s}$ in most areas and may reach $1.25 \times 10^{-3} \text{ mm}^2/\text{s}$ in the posterior periventricular regions with lower WM myelination [120]. Hence calculation of lesion-to-brain ratios, which implies the normalisation of individual data, provides an obvious advantage. While we failed to detect a difference between gliomas, meningiomas and metastases with respect to the ADC values in peritumoral signal changes, conflicting observations can be found in the literature. Krabbe et al. and Lu et al. compared high grade gliomas to metastases and to meningiomas, respectively [94, 95]. Both groups found elevated ADC in the peritumoral area with T2-changes surrounding metastases. In a study that included high and low grade gliomas, meningiomas and metastases, Lu et al. failed to reproduce these findings [96]. This lack of converging evidence suggests that the usefulness of ADC in the characterisation of peritumoral signal changes may be questionable. Values of ADC in adjacent NAWM have been reported by Provenzale et al. [98], who compared gliomas to meningiomas. In gliomas the average ADC in the NAWM adjacent to the tumor ($0.683 \times 10^{-3} \text{ mm}^2/\text{s}$) was decreased as compared to that in the contralateral white matter ($0.723 \times 10^{-3} \text{ mm}^2/\text{s}$). However, this difference falls within the normal range for ADC. We have chosen to attribute the small differences between the ADC values in the adjacent NAWM in our material to the normal variation of ADC in the brain.

FA varies between different regions of the brain and is typically 0.1–0.2 in grey matter, rising to 0.6–0.8 in densely packed white matter bundles such as the corpus callosum [29]. Reports on the use of FA for assessment of tumor extension in gliomas describe a difference between gliomas and meningiomas in peritumoral areas with increased T2 as well as a lack of change between high grade gliomas and metastases [88, 95, 98]. The large variation of FA within the brain may complicate its usefulness in the evaluation of tumor extension. In addition, differences in FA values between tumors of one histological type may in part reflect the primary location of the tumor, since tumor locations vary in clinical materials. While FA may be affected by moderate tumor cell invasion into white matter tracts of high anisotropy such as the corpus callosum, it may still remain higher than in regions with lower FA, such as the optic radiation. Furthermore, high grade gliomas, although similarly classified, may vary in their behavior [37]. For example, some exert a mass effect on the surrounding

tissue resulting in compression of the adjacent white matter while others destruct white matter fibres.

Steroid treatment (dexamethasone) has been reported to reduce ADC in peritumoral areas with T2-signal changes in all three tumor types, by decreasing the water content [121]. As this effect is independent of tumor type, and the treatment was given to 73 % of patients with high grade gliomas and to 75 % of patients with meningiomas or metastases, we assume that steroid treatment has not affected our results. The field strength of 3 T was used in our study. Increased field strength results in higher signal to noise ratios. In addition, the gradients of the new 3 T equipments are higher. These two properties contribute to the usefulness of DTI for measuring small differences in the location of protons in multiple directions. The use of higher field strength for the measurements of ADC and FA can therefore be expected to be appropriate for distinguishing tumor-infiltrated edema in gliomas from pure edema in meningiomas and metastases. Finally, our study as well as work referred to above lacks a direct correlation with histopathology. This should be the final step in evaluating DTI for assessment of tumour spread in high grade gliomas, presumably using stereotactic biopsies or post mortem follow-up.

Future aspects

High grade gliomas, the most common primary brain tumors in adults, remain associated with poor prognosis despite therapeutic advances [122]. MRI with its sensitivity for soft tissue details is the imaging modality of choice as regards diagnosis and monitoring of therapy [41]. The introduction of MRI techniques aiming at measurement of physiologic parameters in vivo has brought the comprehensive neuroradiological workup of patients with intracranial tumors a step beyond conventional MRI including T1- and T2 weighted images before and after contrast enhancement. The use of fMRI and DTI has been described previously in this thesis. Diffusion Weighted Imaging enables the neuroradiologist to differentiate between the putative diagnoses of abscess and tumor, to differ between different tumor types and to evaluate therapy response [123, 124, 91, 125, 126]. Perfusion Weighted Imaging (PWI) mapping cerebral blood flow and blood volume, facilitates the assessment of malignancy in gliomas and aids in the differentiation between radiation necrosis and recurrent tumor [127-130]. Magnetic Resonance Spectroscopy (MRS) allows for differentiation between infiltrating and non-infiltrating intracranial tumors (gliomas and metastases, respectively) [131, 132].

Functional MRI for preoperative mapping of brain functions will become increasingly available due to the increasing number of modern MR scanners. For example, manufacturers deliver new scanners with software for advanced motion correction of functional time series and for real time fMRI, that displays the statistical analysis while the patient is performing the paradigm, to name some examples. The emergence of functional neuroimaging as a significant clinical tool will trigger a growing need for specialized training among neuroradiologists, neurologists and neurosurgeons. Basic understanding of how an fMRI study is performed, paradigm design and data analysis will be required as well as familiarity with the limitations of fMRI and the implications these have when interpreting fMRI results. In the absence

of standardized study protocols, each site establishes its routines as regards MR protocol, stimulation, data analysis and interpretation of activation maps. Quality control aimed at optimizing these procedures for distribution and general use in the clinical functional neuroimaging community is an issue to be addressed in the future. Although the value of DTI for characterisation of tumor edema in gliomas has not been established, other applications may contribute to the preoperative evaluation of patients with intracranial tumors. The principal direction of the diffusion tensor, λ_1 , can be calculated for each voxel. A given voxel can then be connected to an adjacent voxel in accordance with the direction of λ_1 , and thus white matter fibre tracts can be reconstructed [133, 134]. DTI tractography may be of use in combination with fMRI, for example for demonstrating displacement or interruption of fibre tracts closely connected to a functional area. In patients with intracranial tumors where mass effect precludes the identification of functional areas, fMRI might be used to localise the primary motor cortex. DTI can then localise the corticospinal tract, starting from the motor cortex as shown by fMRI [135, 136]. Reports however are largely single-center, uncontrolled, preliminary findings and must be cautiously interpreted and need further evaluation.

In order for MRI to contribute optimally to early diagnosis and adequate therapeutic monitoring of patients with intracranial tumors, a comprehensive work-up that utilizes all available parameters must be developed, validated and optimized. This task will be a challenge for the years to come.

Conclusions

Our results suggest that the spatial resolution of fMRI using a clinical protocol is adequate for localisation of the sensory representation of a finger (Paper 1).

Preoperative fMRI for mapping of motor, sensory and language functions at 3 T is feasible and contributes to neurosurgical decision making (Paper 2).

Longitudinal pre- and postoperative fMRI studies may be performed in patients with gliomas without concerns for potential effects of the decreased tumor volume on the BOLD effect as a possible source of error (Paper 3).

Values and lesion-to-brain ratios of ADC and FA may not be useful to distinguish pure edema from tumor-infiltrated edema in peritumoral areas with T2-signal changes (Paper 4).

Acknowledgements

This work could not have been initiated, carried through and completed without the help, assistance, enthusiasm and support from many. I am grateful to all of you.

Elna-Marie Larsson, associate professor in Neuroradiology and director of MRI at our department, my supervisor who always managed to make me see the potential of this work. Thank you for your enthusiasm and your faith in this project and in me, as well as for your generous support in practical matters

Peter Fransson, associate professor at Karolinska Hospital, Stockholm, co-supervisor of this thesis, for always finding time to answer my questions, and for getting me started with SPM

Johan Olsrud, physicist at our MR department and co-author, who put together the equipment for stimulus presentation and data transfer, for his ever increasing knowledge of fMRI, his friendliness and his patience with my ignorance

My co-authors, *Gunnar Skagerberg*, associate professor at the Department for Neurosurgery, *Birgitta Rosén*, associate professor and *Göran Lundborg*, professor, both at the Department of Hand Surgery, Malmö, *Jimmy Lätt* and *Sara Brockstedt*, both physicists, and *Elisabet Englund*, associate professor at the Department of Neuropathology, for their valuable contributions to this thesis

Fredrik Örtendahl, *Amir Vahabi*, *Siv Tjernström* and *Pia Wejdegård*, technicians at the Allegra MR-scanner, who conducted the fMRI-studies on patients and volunteers, for their professionalism and enthusiasm

Mårten Annertz, *Isabella Björkman-Burtscher*, *Mats Cronquist*, *Åke Forssell*, *Christer Lundahl*, *Cecilia Petersen*, *Birgitta Ramgren*, *Roger Siemund*, *Lars Stenberg* and *Per Undrén*, my colleagues at the Department of Neuroradiology, for understanding and support

Holger Pettersson, professor at the Department of Radiology and *Peter Hochbergs*, head of the Center for Medical Imaging and Physiology, for giving me resources to do this work

The physics group at the Institution of Radiation Physics, lead by professor *Freddy Ståhlberg*, for their interest and support

All personnel at the MR-department for being positive and encouraging

Anita Sundström and *Eva Jönsson*, our secretaries, for skilful assistance

The *Swedish Medical Research Council*, the *Medical Faculty at Lund University*, the *Skåne County Council Research and Development Foundation*, the *Segeffalk Foundation* and the *Royal Physiographic Society* in Lund for financial support

Christina Elfgren, neuropsychologist and associate professor, for friendship and inspiration

Friends near and far, for patience and interest

My family in Holland, my parents, my brother and sister, their partners, their children, as well as in Sweden, Sofies parents, sisters and brother, their partners and their children, for being by my side

Nina and Paula, my daughters, for being there, which is a miracle every morning

Sofie, the big 'L' for Love, for encouragement, advice, patience with some things and impatience with others, for guiding me through when the going is tough and never making me lose sight of what really matters

References

1. Bloch F, Hansen WW, Packard M. The nuclear induction experiment. *Physical review* 1946;70:474-85.
2. Purcell EM, Torrey HC, Pound RV. Resonance absorption by nuclear magnetic moments in a solid. *Physical review* 1946;69:37-8.
3. Lauterbur PC. Image formation by induced local interactions: examples employing nuclear magnetic resonance. *Nature* 1973;242:190-1.
4. Damadian RV. Tumor detection by NMR. *Science* 1971;171:1151-53.
5. Roy CS, Sherrington CS. On the regulation of the blood-supply of the brain. *J Physiol* 1890;11:85-108.
6. Pauling L, Coryell C. The magnetic properties and structure of haemoglobin, oxyhemoglobin, and carbon monoxyhemoglobin. *Proc. Natl Acad Sci U S A* 1936;22:210-6
7. Malonek D, Dirnagl U, Lindauer U, Yamada K, Kanno I, Grinvald A. Vascular imprints of neuronal activity: relationships between the dynamics of cortical blood flow, oxygenation, and volume changes following sensory stimulation. *Proc. Natl Acad Sci U S A* 1997;94:14826-31.
8. Thulborn KR, Waterton JC, Matthews PM, Radda GK. Oxygenation dependence of the transverse relaxation time of water protons in whole blood at high field. *Biochim Biophys Acta* 1982;714:265-70.
9. Ogawa S, Tank DW, Menon R, Ellermann JM, Kim SG, Merkle H, Ugurbil K. Intrinsic signal changes accompanying sensory stimulation: functional brain mapping with magnetic resonance imaging. *Proc. Natl Acad Sci U S A* 1992 1;89:5951-5.
10. Kwong KK, Belliveau JW, Chesler DA, Goldberg IE, Weisskoff RM, Poncelet BP, Kennedy DN, Hoppel BE, Cohen MS, Turner R, Cheng H, Brady TJ, Rosen B.. Dynamic magnetic resonance imaging of human brain activity during primary sensory stimulation. *Proc Natl Acad Sci U S A*. 1992 15;89:5675-9.
11. Ogawa S, Lee TM, Kay AR, Tank DW. Brain magnetic resonance imaging with contrast dependent on blood oxygenation. *Proc. Natl Acad Sci U S A* 1990;87:9868-72.
12. Rees G, Friston K, Koch C. A direct quantitative relationship between the functional properties of human and macaque V5. *Nat Neurosci*. 2000;3:716-23.
13. Buxton RB, Wong EC, Frank LR. Dynamics of blood flow and oxygenation changes during brain activation: the balloon model. *Magn Reson Med* 1998;39:855-64.
14. Mandeville JB, Marota JJ, Ayata C, Moskowitz MA, Weisskoff RM, Rosen BR. MRI measurement of the temporal evolution of relative CMRO(2) during rat forepaw stimulation. *Magn Reson Med* 1999;42:944-51.
15. Mansfield P. Multi-planar image formation using NMR spin echoes. *J Physiol Chem* 1977;10: L55-8.

16. Edelstein WA, Glover GH, Hardy CJ, Redington RW. The intrinsic signal-to-noise ratio in NMR imaging. *Magn Res Med* 1986;3:604-18.
17. Hoult DI, Lauterbur PC. The sensitivity of the zeugmatographic experiment involving human samples. *J Magn Res* 1979;34:425-33.
18. Gati JS, Menon RS, Ugurbil K, Rutt BK. Experimental determination of the BOLD field strength dependence in vessels and tissue. *Magn Res Med* 1997 Aug;38(2):296-302.
19. Okada T, Yamada H, Ito H, Yonekura Y, Sadato N. Magnetic field strength increase yields significantly greater contrast-to-noise ratio increase: Measured using BOLD contrast in the primary visual area. *Acad Radiol* 2005;12:142-7.
20. Statistical Parametric Mapping (<http://www.fil.ion.ucl.ac.uk/spm>)
21. Brain Voyager (<http://www.brainvoyager.com>)
22. Friston KJ, Ashburner J, Frith CD, Poline JB, Heather JD, Frackowiak RSJ. Spatial registration and normalization of images. *Hum Brain Mapp* 1995;2:165-89.
23. Friston KJ, Jezzard PJ, Turner R. Analysis of functional MRI time-series *Hum Brain Mapp* 1994;1:153-71
24. Friston KJ, Holmes AP, Worsley KJ, Poline JB, Frith CD, Frackowiak RSJ. Statistical Parametric Maps in functional imaging: A general linear approach *Hum Brain Mapp* 1995;2:189-210.
25. Bandettini PA, Jesmanowicz A, Wong EC, Hyde JS. Processing strategies for time-course data sets in functional MRI of the human brain. *Magn Reson Med*. 1993;30:161-73.
26. Le Bihan D, Breton E, Lallemand D, Grenier P, Cabanis E, Laval-Jeantet M. MR imaging of intravoxel incoherent motions: application to diffusion and perfusion in neurologic disorders. *Radiology* 1986;161:401-7.
27. Turner R, Le Bihan D, Maier J, Vavrek R, Hedges LK, Pekar J. Echo-planar imaging of intravoxel incoherent motion. *Radiology* 1990;177:407-14.
28. Chenevert TL, Brunberg JA, Pipe JG. Anisotropic diffusion in human white matter: demonstration with MR techniques in vivo. *Radiology* 1990;177:401-5.
29. Pierpaoli C, Basser PJ. Toward a quantitative assesment of diffusion anisotropy. *Magn Reson Med* 1996;36:893-906.
30. Stejskal E, Tanner J. Spin diffusion measurements: spin echoes in the presence of time-dependent field gradient. *J Chem Phys* 1965;42:288-92.
31. Warach S, Chien D, Li W, Ronthal M, Edelman RR. Fast magnetic resonance diffusion-weighted imaging of acute human stroke. *Neurology* 1992;42:1717-23.
32. Sunshine JL, Tarr RW, Lanzieri CF, Landis DM, Selman WR, Lewin JS. Hyperacute stroke: ultrafast MR imaging to triage patients prior to therapy. *Radiology* 1999;212:325-32.
33. Stadnik TW, Chaskis C, Michotte A, Shabana WM, van Rompaey K, Luypaert R, Budinsky L, Jellus V, Osteaux M. Diffusion-weighted MR imaging of intracerebral masses: comparison with conventional MR imaging and histologic findings. *Am J Neuroradiol* 2001;22:969-76.

34. Basser PJ, Mattiello J, Le Bihan D. MR diffusion tensor spectroscopy and imaging. *Biophys J* 1994;66:256-67.
35. Basser PJ, Pierpaoli C. Microstructural and physiological features of tissues elucidated by quantitative-diffusion-tensor MRI. *J Magn Reson B* 1996;111:209-19.
36. Basser PJ. Inferring microstructural features and the physiological state of tissues from diffusion-weighted images. *NMR Biomed* 1995;8:333-44.
37. Kleihues P and Cavenee WK, eds. *Tumours of the Nervous System. Pathology and Genetics. The WHO Classification of Tumours.* International Agency for Research on Cancer Press, Lyon, France, 2000.
38. Levin VA, Leibel SA, Gutin PH Neoplasms of the central nervous system. In: DeVita VT Jr, Hellman S, Rosenberg SA, eds.: *Cancer: Principles and Practice of Oncology.* 6th ed. Philadelphia, Pa: Lippincott Williams & Wilkins, 2001, pp 2100-60.
39. Kleihues P, Burger PC, Collins VP, et al. Glioblastoma. In: Kleihues P, Cavenee WK, eds.: *Pathology and Genetics of Tumours of the Nervous System.* Lyon, France: International Agency for Research on Cancer, 2000, pp 29-39.
40. Posner JB. Management of brain metastases. *Rev Neurol* 1992;148:477-87.
41. Atlas SW, Lavi E, Fisher PG. Intraaxial Brain Tumors. In: Atlas SW, ed. *Magnetic resonance of the brain and spine.* 3rd ed. Lippincott, Williams & Wilkins, Philadelphia, USA, 2002, pp 565-693.
42. Atlas SW, Lavi E, Goldberg HI. Extraaxial Brain Tumors. In: Atlas SW, ed. *Magnetic resonance of the brain and spine.* 3rd ed. Lippincott, Williams & Wilkins, Philadelphia, USA, 2002, pp 695-772.
43. Keles GE, Lamborn KR, Berger MS. Low-grade hemispheric gliomas in adults: a critical review of extent of resection as a factor influencing outcome. *J Neurosurg.* 2001;95:735-45.
44. Claus EB, Black PM. Survival rates and patterns of care for patients diagnosed with supratentorial low-grade gliomas: data from the SEER program, 1973-2001. *Cancer.* 2006;15:1358-63.
45. Simpson JR, Horton J, Scott C, Curran WJ, Rubin P, Fischbach J, Isaacson S, Rotman M, Asbell SO, Nelson JS Influence of location and extent of surgical resection on survival of patients with glioblastoma multiforme: results of three consecutive Radiation Therapy Oncology Group (RTOG) clinical trials. *Int J Radiat Oncol Biol Phys.* 1993;20:239-44
46. Reardon DA, Rich JN, Friedman HS, Bigner DD. Recent advances in the treatment of malignant astrocytoma. *J Clin Oncol.* 2006;24:1253-65.
47. McMullen KP, Stieber VW. Meningioma: current treatment options and future directions. *Curr Treat Options Oncol.* 2004 Dec;5(6):499-509
48. Vogelbaum MA, Suh JH. Resectable brain metastases. *J Clin Oncol.* 2006 Mar 10;24(8):1289-94.
49. Cabeza R, Nyberg L. Imaging cognition II: An empirical review of 275 PET and fMRI studies. *J Cogn Neurosci.* 2000 Jan;12(1):1-47.

50. Brannen JH, Badie B, Moritz CH, Quigley M, Meyerand ME, Haughton VM. Reliability of functional MR imaging with word-generation tasks for mapping Broca's area. *Am J Neuroradiol* 2001;22:1711-8.
51. Fandino J, Kollias SS, Wieser HG, Valavanis A, Yonekawa Y. Intraoperative validation of functional magnetic resonance imaging and cortical reorganization patterns in patients with brain tumors involving the primary motor cortex. *J Neurosurg* 1999;91:238-50.
52. FitzGerald DB, Cosgrove GR, Ronner S, Jiang H, Buchbinder BR, Belliveau JW, Rosen BR. Location of language in the cortex: a comparison between functional MR imaging and electrocortical stimulation. *Am J Neuroradiol* 1997; 18:1529-39.
53. Krings T, Schreckenberger M, Rohde V, Spetzger U, Sabri O, Reinges MH, Hans FJ, Meyer PT, Moller-Hartmann W, Gilsbach JM, Buell U, Thron A. Functional MRI and 18F FDG-positron emission tomography for presurgical planning: comparison with electrical cortical stimulation. *Acta Neurochir (Wien)* 2002;144:889-99.
54. L  h  ricy S, Duffau H, Cornu P, Capelle L, Pidoux B, Carpentier A, Auliac S, Clemenceau S, Sichez JP, Bitar A, Valery CA, Van Effenterre R, Faillot T, Srouf A, Fohanno D, Philippon J, Le Bihan D, Marsault C. Correspondence between functional magnetic resonance imaging somatotopy and individual brain anatomy of the central region: comparison with intraoperative stimulation in patients with brain tumors. *J Neurosurg* 2000 92:589-98.
55. Mueller WM, Yetkin FZ, Hammeke TA, Morris GL, Swanson SJ, Reichert K, Cox R, Haughton VM. Functional magnetic resonance imaging mapping of the motor cortex in patients with cerebral tumors. *Neurosurgery* 1996;39:515-20.
56. Pujol J, Conesa G, Deus J, Lopez-Obarrio L, Isamat F, Capdevila A. Clinical application of functional magnetic resonance imaging in presurgical identification of the central sulcus. *J Neurosurg* 1998;88:863-9.
57. Roux FE, Boulanouar K, Ranjeva JP, Manelfe C, Tremoulet M, Sabatier J, Berry I. Cortical intraoperative stimulation in brain tumors as a tool to evaluate spatial data from motor functional MRI. *Invest Radiol* 1999;34:225-9.
58. Roux FE, Boulanouar K, Lotterie JA, Mejdoubi M, LeSage JP, Berry I. Language functional magnetic resonance imaging in preoperative assessment of language areas: correlation with direct cortical stimulation. *Neurosurgery*. 2003 Jun;52(6):1335-45; discussion 1345-7.
59. Schlosser MJ, Luby M, Spencer DD, Awad IA, McCarthy G. Comparative localization of auditory comprehension by using functional magnetic resonance imaging and cortical stimulation. *J Neurosurg* 1999;91:626-35.
60. Yetkin FZ, Mueller WM, Morris GL, McAuliffe TL, Ulmer JL, Cox RW, Daniels DL, Haughton VM. Functional MR activation correlated with intraoperative cortical mapping. *Am J Neuroradiol* 1997;18:1311-5.
61. Ajmani RS, Metter EJ, Jaykumar R, Ingram DK, Spangler EL, Abugo OO, Rifkind JM. Hemodynamic changes during aging associated with cerebral blood flow and impaired cognitive function. *Neurobiol Aging*. 2000;21:257-69.

62. Cabeza R, Nyberg L. Imaging Cognition: An Empirical Review of PET Studies with Normal Subjects. *J Cogn Neurosci* 1997; 9:1-26.
63. Watanabe M, Tanaka R, Takeda N. Magnetic resonance imaging and histopathology of cerebral gliomas. *Neuroradiology* 1992;34:463-9
64. Kelly PJ, Dumas-Duport C, Kispert DB, Kall BA, Scheithauer BW, Illig JJ. Imaging-based stereotaxic serial biopsies in untreated intracranial glial neoplasms. *J Neurosurg* 1987;66:865-74.
65. Menon RS, Ogawa S, Strupp JP, Ugurbil K. Ocular dominance in human V1 demonstrated by functional magnetic resonance imaging. *J Neurophysiol.* 1997;77:2780-7.
66. Gardner EP, Kandel ER. Touch. In: Kandel ER, Schwartz JH, Jessell TM eds. *Principles of Neural Science*. McGraw-Hill, 2000, New York, USA 2000, pp 451-71.
67. Yousry TA, Schmid UD, Alkadhi H, Schmidt D, Peraud A, Buettner A, Winkler P. Localization of the motor hand area to a knob on the precentral gyrus. A new landmark. *Brain* 1997;120:141-57.
68. Kaas JH, Nelson RJ, Sur M, Lin CS, Merzenich MM. Multiple representations of the body within the primary somatosensory cortex of primates. *Science* 1979;204:521-3.
69. Gelnar PA, Krauss BR, Szeverenyi NM, Apkarian AV. Fingertip representation in the human somatosensory cortex: an fMRI study. *NeuroImage* 1998;7:261-83.
70. Maldjian JA, Gottschalk A, Patel RS, Detre JA, Alsop DC. The sensory somatotopic map of the human hand demonstrated at 4 Tesla. *NeuroImage* 1999;10:55-62.
71. Kurth R, Villringer K, Mackert BM, Schwiemann J, Braun J, Curio G, Villringer A, Wolf KJ. fMRI assessment of somatotopy in human Brodmann area 3b by electrical finger stimulation. *NeuroReport* 1998;9:207-12.
72. Kurth R, Villringer K, Curio G, Wolf KJ, Krause T, Repenthin J, Schwiemann J, Deuchert M, Villringer A. fMRI shows multiple somatotopic digit representations in human primary somatosensory cortex. *NeuroReport* 2000;11:1487-91.
73. Stippich C, Kapfer D, Hempel E, Borgulya G, Bongers A, Heiland S, Sartor K. Robust localization of the contralateral precentral gyrus in hemiparetic patients using the unimpaired ipsilateral hand: a clinical functional magnetic resonance imaging protocol. *Neurosci Lett.* 2000;12:155-9.
74. Vlioger EJ, Majoie CB, Leenstra S, Den Heeten GJ. Functional magnetic resonance imaging for neurosurgical planning in neurooncology. *Eur Radiol.* 2004;14:1143-53.
75. Hirsch J, Ruge MI, Kim KH, Correa DD, Victor JD, Relkin NR, Labar DR, Krol G, Bilsky MH, Souweidane MM, DeAngelis LM, Gutin PH. An integrated functional magnetic resonance imaging procedure for preoperative mapping of cortical areas associated with tactile, motor, language, and visual functions. *Neurosurgery.* 2000;47:711-21.

76. Krings T, Reinges MH, Erberich S, Kemeny S, Rohde V, Spetzger U, Korinth M, Willmes K, Gilsbach JM, Thron A.. Functional MRI for presurgical planning: problems, artefacts, and solution strategies. *J Neurol Neurosurg Psychiatry* 2001;70:749-60.
77. Hinke RM, Hu X, Stillman AE, Kim SG, Merkle H, Salmi R, Ugurbil K. Functional magnetic resonance imaging of Broca's area during internal speech. *Neuroreport* 1993;4:675-8.
78. Phelps EA, Hyder F, Blamire AM, Shulman RG. FMRI of the prefrontal cortex during overt verbal fluency. *Neuroreport* 1997;20:561-5.
79. Lee CC, Ward HA, Sharbrough FW, Meyer FB, Marsh WR, Raffel C, , So EL, Cascino GD, Shin C, Xu Y, Riederer SJ, Jack CR.. Assessment of functional MR imaging in neurosurgical planning. *Am J Neuroradiol* 1999;20(8):1511-9.
80. Haberg A, Kvistad KA, Unsgard G, Haraldseth O. Preoperative blood oxygen level-dependent functional magnetic resonance imaging in patients with primary brain tumors: clinical application and outcome. *Neurosurgery* 2004;54:902-14.
81. Haglund MM, Berger MS, Shamseldin M, Lettich E, Ojemann GA. Cortical localization of temporal lobe language sites in patients with gliomas. *Neurosurgery* 1994;34:567-76.
82. Holodny AI, Schulder M, Liu WC, Maldjian JA, Kalnin AJ. Decreased BOLD functional MR activation of the motor and sensory cortices adjacent to a glioblastoma multiforme: implications for image-guided neurosurgery. *Am J Neuroradiol* 1999;20:609-12.
83. Schreiber A, Hubbe U, Ziyeh S, Hennig J. The influence of gliomas and nonglial space-occupying lesions on blood-oxygen-level-dependent contrast enhancement. *Am J Neuroradiol* 2000;21:1055-63.
84. Schlosser R, Hunsche S, Gawehn J, Grunert P, Vucurevic G, Gesierich T, Kaufmann B, Rossbach W, Stoeter P. Characterization of BOLD-fMRI signal during a verbal fluency paradigm in patients with intracerebral tumors affecting the frontal lobe. *Magn Reson Imaging* 2002;20:7-16.
85. Ojemann JG, Neil JM, MacLeod AM, Silbergeld DL, Dacey RG Jr, Petersen SE, Raichle ME. Increased functional vascular response in the region of a glioma. *J Cereb. Blood Flow Metab* 1998;18:148-53.
86. Yetkin FZ, McAuliffe TL, Cox R, Haughton VM. Test-retest precision of functional MR in sensory and motor task activation. *Am J Neuroradiol* 1996;17:95-8.
87. Rutten GJ, Ramsey NF, van Rijen PC, van Veelen CW. Reproducibility of fMRI-determined language lateralization in individual subjects. *Brain Lang* 2002 80:421-37.
88. Bastin ME, Sinha S, Whittle IR, Wardlaw JM. Measurements of water diffusion and T1 values in peritumoral oedematous brain. *Neuroreport* 2002;13:1335-40.
89. Castillo M, Smith JK, Kwock L, Wilber K. Apparent diffusion coefficients in the evaluation of high-grade cerebral gliomas. *Am J Neuroradiol* 2001;22:60-4.

90. Field AS, Alexander AL, Wu YC, Hasan KM, Witwer B, Badie B. Diffusion tensor eigenvector directional color imaging patterns in the evaluation of cerebral white matter tracts altered by tumor. *J Magn Reson Imaging* 2004;20:555-62.
91. Gauvain KM, McKinstry RC, Mukherjee P, Perry A, Neil JJ, Kaufman BA, Hayashi RJ. Evaluating pediatric brain tumor cellularity with diffusion-tensor imaging. *Am J Roentgenol* 2001;177:449-54.
92. Guo AC, Cummings TJ, Dash RC, Provenzale JM. Lymphomas and high grade gliomas: comparison of water diffusibility and histologic characteristics. *Radiology* 2002;224:177-83.
93. Kono K, Inoue Y, Nakayama K, Shakudo M, Morino M, Ohata K, Wakasa K, Yamada R. The role of diffusion-weighted imaging in patients with brain tumors. *Am J Neuroradiol* 2001;22:1081-8.
94. Krabbe K, Gideon P, Wagn P, Hansen U, Thomsen C, Madsen F. MR diffusion imaging of human intracranial tumors. *Neuroradiology* 1997;39:483-9.
95. Lu S, Ahn D, Johnson G, Cha S. Peritumoral diffusion tensor imaging of high-grade gliomas and metastatic brain tumors. *Am J Neuroradiol* 2003;24:937-41.
96. Lu S, Ahn D, Johnson G, Law M, Zagzag D, Grossman RI. Diffusion-tensor MR imaging of intracranial neoplasia and associated peritumoral edema: introduction of the tumor infiltration index. *Radiology* 2004;232:221-8.
97. Price SJ, Burnet NG, Donovan T, Green HA, Pena A, Antoun NM, Pickard JD, Carpenter TA, Gillard JH. Diffusion tensor imaging of brain tumors at 3T: a potential tool for assessing white matter tract invasion? *Clin Radiol* 2003;58:455-62.
98. Provenzale JM, McGraw P, Mhatre P, Guo AC, Delong D. Peritumoral brain regions in gliomas and meningiomas: investigation with isotropic diffusion-weighted MR imaging and diffusion-tensor MR imaging. *Radiology* 2004;232:451-60.
99. Sinha S, Bastin ME, Whittle IR, Wardlaw JM. Diffusion tensor MR imaging of high-grade cerebral gliomas. *Am J Neuroradiol* 2002;23:520-27.
100. Stadnik TW, Chaskis C, Michotte A, Shabana WM, van Rompaey K, Luybaert R, Budinsky L, Jellus V, Osteaux M. Diffusion-weighted MR imaging of intracerebral masses: comparison with conventional MR imaging and histologic findings. *Am J Neuroradiol* 2001;22:969-76.
101. Tropine A, Vucurevic G, Delani P, Boor S, Hopf N, Bohl J, Stoeter P. Contribution of diffusion tensor imaging to delineation of gliomas and glioblastomas. *J Magn Reson Imaging* 2004;20:905-12.
102. Geyer S, Schleicher A, Zilles K. Areas 3a, 3b, and 1 of human primary somatosensory cortex. *Neuroimage* 1999;10:63-83.
103. Geyer S, Schormann T, Mohlberg H, Zilles K. Areas 3a, 3b, and 1 of human primary somatosensory cortex. Part 2. Spatial normalization to standard anatomical space. *Neuroimage* 2000;11:684-96.

104. Thesen S, Heid O, Mueller E, Schad LR. Prospective acquisition correction for head motion with image-based tracking for real-time fMRI. *Magn Reson Med* 2000; 44:457-65.
105. Hertz-Pannier L, Gaillard WD, Mott SH, Cuenod CA, Bookheimer SY, Weinstein S, Conry J, Papero PH, Schiff SJ, Le Bihan D, Theodore WH. Noninvasive assessment of language dominance in children and adolescents with functional MRI: a preliminary study. *Neurology* 1997;48:1003-12
106. Yang Y, Wen H, Mattay VS, Balaban RS, Frank JA, et al. Comparison of 3D BOLD functional MRI with spiral acquisition at 1.5 and 4.0 T. *Neuroimage* 1999;9:446-51.
107. Kruger G, Kastrup A, Glover GH. Neuroimaging at 1.5 T and 3.0 T: comparison of oxygenation-sensitive magnetic resonance imaging. *Magn Reson Med* 2001;45:595-604.
108. Krasnow B, Tamm L, Greicius MD, Yang TT, Glover GH, Reiss AL, Menon V. Comparison of fMRI activation at 3 and 1.5 T during perceptual, cognitive, and affective processing. *Neuroimage*. 2003;18:813-26.
109. Hoenig K, Kuhl CK, Scheef L. Functional 3.0-T MR assessment of higher cognitive function: Are there advantages over 1.5-T imaging? *Radiology* 2005;234: 860-8.
110. Ogawa S, Menon RS, Tank DW, Kim SG, Merkle H, Ellermann JM, Ugurbil K. Functional brain mapping by blood oxygenation level-dependent contrast magnetic resonance imaging. A comparison of signal characteristics with a biophysical model. *Biophys J* 1993;64:803-12.
111. Fisel CR, Ackerman JL, Buxton RB, Garrido L, Belliveau JW, Rosen BR, Brady TJ. MR contrast due to microscopically heterogeneous magnetic susceptibility: numerical simulations and applications to cerebral physiology. *Magn Reson Med* 1991;17:336-47.
112. Merzenich MM, Kaas JH, Sur M, Lin CS. Double representation of the body surface within cytoarchitectonic areas 3b and 1 in "SI" in the owl monkey (*Aotus trivirgatus*). *J Comp Neurol* 1978;181:41-73.
113. Hari R, Karhu J, Hamalainen M, Knuutila J, Salonen O, Sams M, Vilkmann V: Functional organization of the human first and second somatosensory cortices: a neuromagnetic study. *Eur J Neurosci* 1993;5:724-34.
114. Buchner H, Fuchs M, Wischmann HA, Dossel O, Ludwig I, Knepper A, Berg P: Source analysis of median nerve and finger stimulated somatosensory evoked potentials: multichannel simultaneous recording of electric and magnetic fields combined with 3D-MR tomography. *Brain Topogr* 1994; 6:299-310.
115. Buchner H, Adams L, Muller A, Ludwig I, Knepper A, Thron A, Niemann K, Scherg M. Somatotopy of human hand somatosensory cortex revealed by dipole source analysis of early somatosensory evoked potentials and 3D-NMR tomography. *Electroencephalogr Clin Neurophysiol* 1995;96:121-34.
116. Boakye M, Huckins SC, Szeverenyi NM, Taskey BI, Hodge CJ Jr. Functional magnetic resonance imaging of somatosensory cortex activity produced by

- electrical stimulation of the median nerve or tactile stimulation of the index finger. *J Neurosurg* 2000;93:774-83.
117. Mannfolk P, van Westen D, Larsson E-M, Olsrud J. Mapping the effects of magnetic field inhomogeneity in EPI for fMRI. ESMRMB 20th annual meeting, September 17-20 2003, Rotterdam, The Netherlands.
 118. Krishnan R, Raabe A, Hattingen E, Szelenyi A, Yahya H, Hermann E, Zimmermann M, Seifert V. Functional magnetic resonance imaging-integrated neuronavigation: correlation between lesion-to-motor cortex distance and outcome. *Neurosurgery* 2004;55:904-14.
 119. Kokkonen SM, Kiviniemi V, Makiranta M, Yrjana S, Koivukangas J, Tervonen O. Effect of brain surgery on auditory and motor cortex activation: a preliminary functional magnetic resonance imaging study. *Neurosurgery* 2005;57:249-56.
 120. Sener RN. Diffusion MRI: apparent diffusion coefficient (ADC) values in the normal brain and a classification of brain disorders based on ADC values. *Comput Med Imaging Graph* 2001;25:299-326.
 121. Sinha S, Bastin ME, Wardlaw JM, Armitage PA, Whittle IR. Effects of dexamethasone on peritumoural oedematous brain: a DT-MRI study. *J Neurol Neurosurg Psychiatry* 2004;75:1632-5.
 122. Legler JM, Ries LA, Smith MA. Cancer surveillance series corrected: brain and other central nervous system cancers: recent trends in incidence and mortality. *J Natl Cancer Inst* 1999;91:1382-1390.
 123. Ebisu T, Tanaka C, Umeda M, Kitamura M, Naruse S, Higuchi T, Ueda S, Sato H. Discrimination of brain abscess from necrotic or cystic tumors by diffusion-weighted echo planar imaging. *Magn Reson Imaging*. 1996;14:1113-6.
 124. Kim YJ, Chang KH, Song IC, Kim HD, Seong SO, Kim YH, Han MH. Brain abscess and necrotic or cystic brain tumor: discrimination with signal intensity on diffusion-weighted MR imaging. *AJR Am J Roentgenol*. 1998;171:1487-90.
 125. Hamstra DA, Chenevert TL, Moffat BA, Johnson TD, Meyer CR, Mukherji SK, Quint DJ, Gebarski SS, Fan X, Tsien CI, Lawrence TS, Junck L, Rehemtulla A, Ross BD. Evaluation of the functional diffusion map as an early biomarker of time-to-progression and overall survival in high-grade glioma. *Proc Natl Acad Sci U S A*. 2005;102:16759-64.
 126. Moffat BA, Chenevert TL, Lawrence TS, Meyer CR, Johnson TD, Dong Q, Tsien C, Mukherji S, Quint DJ, Gebarski SS, Robertson PL, Junck LR, Rehemtulla A, Ross BD. Functional diffusion map: a noninvasive MRI biomarker for early stratification of clinical brain tumor response. *Proc Natl Acad Sci U S A*. 2005;102:5524-9.
 127. Aronen HJ, Gazit IE, Louis DN, Buchbinder BR, Pardo FS, Weisskoff RM, Harsh GR, Cosgrove GR, Halpern EF, Hochberg FH. Cerebral blood volume maps of gliomas: comparison with tumor grade and histologic findings. *Radiology* 1994;191:41-51.

128. Knopp EA, Cha S, Johnson G, Mazumdar A, Golfinos JG, Zagzag D, Miller DC, Kelly PJ, Kricheff II. Glial neoplasms: dynamic contrast-enhanced T2*-weighted MR imaging. *Radiology* 1999;211:791-8.
129. Sugahara T, Korogi Y, Kochi M, Ikushima I, Hirai T, Okuda T, Shigematsu Y, Liang L, Ge Y, Ushio Y, Takahashi M. Correlation of MR imaging-determined cerebral blood volume maps with histologic and angiographic determination of vascularity of gliomas. *AJR Am J Roentgenol.* 1998;171:1479-86.
130. Sugahara T, Korogi Y, Tomiguchi S, Shigematsu Y, Ikushima I, Kira T, Liang L, Ushio Y, Takahashi M. Posttherapeutic intraaxial brain tumor: the value of perfusion-sensitive contrast-enhanced MR imaging for differentiating tumor recurrence from nonneoplastic contrast-enhancing tissue. *AJNR Am J Neuroradiol.* 2000;21:901-9.
131. Burtscher IM, Skagerberg G, Geijer B, Englund E, Stahlberg F, Holtas S. Proton MR spectroscopy and preoperative diagnostic accuracy: an evaluation of intracranial mass lesions characterized by stereotactic biopsy findings. *AJNR Am J Neuroradiol.* 2000;21:84-93.
132. Burtscher IM, Holtas S. Proton magnetic resonance spectroscopy in brain tumours: clinical applications. *Neuroradiology.* 2001 May;43(5):345-52.
133. Basser PJ, Pajevic S, Pierpaoli C, Duda J, Aldroubi A. In vivo fiber tractography using DT-MRI data. *Magn Reson Med.* 2000 Oct;44(4):625-32.
134. Mamata H, Mamata Y, Westin CF, Shenton ME, Kikinis R, Jolesz FA, Maier SE. High-resolution line scan diffusion tensor MR imaging of white matter fiber tract anatomy. *Am J Neuroradiol* 2002;23:67-75.
135. Holodny AI, Ollenschleger MD, Liu WC, Schulder M, Kalnin AJ. Identification of the corticospinal tracts achieved using blood-oxygen-level-dependent and diffusion functional MR imaging in patients with brain tumors. *Am J Neuroradiol* 2001;22:83-8.
136. Guye M, Parker GJ, Symms M, Boulby P, Wheeler-Kingshott CA, Salek-Haddadi A, Barker GJ, Duncan JS. Combined functional MRI and tractography to demonstrate the connectivity of the human primary motor cortex in vivo. *Neuroimage.* 2003;19:1349-60.